

Deep Learning-Based Human Pose Estimation: A Survey

CE ZHENG*, University of Central Florida, USA

WENHAN WU*, University of North Carolina at Charlotte, USA

CHEN CHEN, University of Central Florida, USA

TAOJIANNAN YANG, University of Central Florida, USA

SIJIE ZHU, University of Central Florida, USA

JU SHEN, University of Dayton, USA

NASSER KEHTARNAVAZ, University of Texas at Dallas, USA

MUBARAK SHAH, University of Central Florida, USA

Human pose estimation aims to locate the human body parts and build human body representation (e.g., body skeleton) from input data such as images and videos. It has drawn increasing attention during the past decade and has been utilized in a wide range of applications including human-computer interaction, motion analysis, augmented reality, and virtual reality. Although the recently developed deep learning-based solutions have achieved high performance in human pose estimation, there still remain challenges due to insufficient training data, depth ambiguities, and occlusion. The goal of this survey paper is to provide a comprehensive review of recent deep learning-based solutions for both 2D and 3D pose estimation via a systematic analysis and comparison of these solutions based on their input data and inference procedures. More than 250 research papers since 2014 are covered in this survey. Furthermore, 2D and 3D human pose estimation datasets and evaluation metrics are included. Quantitative performance comparisons of the reviewed methods on popular datasets are summarized and discussed. Finally, the challenges involved, applications, and future research directions are concluded. A regularly updated project page is provided: <https://github.com/zczcwh/DL-HPE>

CCS Concepts: • **Computing methodologies** → **Artificial intelligence; Computer vision.**

Additional Key Words and Phrases: Survey of human pose estimation, 2D and 3D pose estimation, deep learning-based pose estimation, pose estimation datasets, pose estimation metrics

ACM Reference Format:

Ce Zheng, Wenhan Wu, Chen Chen, Taojiannan Yang, Sijie Zhu, Ju Shen, Nasser Kehtarnavaz, and Mubarak Shah. 2018. Deep Learning-Based Human Pose Estimation: A Survey. *J. ACM* 37, 4, Article 111 (August 2018), 35 pages. <https://doi.org/10.1145/1122445.1122456>

*Both authors contributed equally to this research.

Authors' addresses: Ce Zheng, cezhang@knights.ucf.edu, University of Central Florida, Orlando, Florida, USA; Wenhan Wu, University of North Carolina at Charlotte, Charlotte, North Carolina, USA, wwu25@uncc.edu; Chen Chen, University of Central Florida, Orlando, Florida, USA, chen.chen@crvc.ucf.edu; Taojiannan Yang, University of Central Florida, Orlando, Florida, USA, taoyang1122@knights.ucf.edu; Sijie Zhu, University of Central Florida, Orlando, Florida, USA, sizhu@knights.ucf.edu; Ju Shen, University of Dayton, Dayton, Ohio, USA, jshen1@udayton.edu; Nasser Kehtarnavaz, University of Texas at Dallas, Richardson, Texas, USA, kehtar@utdallas.edu; Mubarak Shah, University of Central Florida, Orlando, Florida, USA, shah@crvc.ucf.edu.

Permission to make digital or hard copies of all or part of this work for personal or classroom use is granted without fee provided that copies are not made or distributed for profit or commercial advantage and that copies bear this notice and the full citation on the first page. Copyrights for components of this work owned by others than ACM must be honored. Abstracting with credit is permitted. To copy otherwise, or republish, to post on servers or to redistribute to lists, requires prior specific permission and/or a fee. Request permissions from permissions@acm.org.

© 2018 Association for Computing Machinery.

0004-5411/2018/8-ART111 \$15.00

<https://doi.org/10.1145/1122445.1122456>

1 INTRODUCTION

Human pose estimation (HPE), which has been extensively studied in computer vision literature, involves estimating the configuration of human body parts from input data captured by sensors, in particular images and videos. HPE provides geometric and motion information of the human body which has been applied to a wide range of applications (e.g., human-computer interaction, motion analysis, augmented reality (AR), virtual reality (VR), healthcare, etc.). With the rapid development of deep learning solutions in recent years, such solutions have been shown to outperform classical computer vision methods in various tasks including image classification [110], semantic segmentation [143], and object detection [203]. Significant progress and remarkable performance have already been made by employing deep learning techniques in HPE tasks. However, challenges such as occlusion, insufficient training data, and depth ambiguity still pose difficulties to be overcome. 2D HPE from images and videos with 2D pose annotations is easily achievable and high performance has been reached for the human pose estimation of a single person using deep learning techniques. More recently, attention has been paid to highly occluded multi-person HPE in complex scenes. In contrast, for 3D HPE, obtaining accurate 3D pose annotations is much more difficult than its 2D counterpart. Motion capture systems can collect 3D pose annotation in controlled lab environments; however, they have limitations for in-the-wild environments. For 3D HPE from monocular RGB images and videos, the main challenge is depth ambiguities. In a multi-view settings, viewpoints association is the key issue that needs to be addressed. Some works have utilized sensors such as depth sensor, inertial measurement units (IMUs), and radio frequency devices, but these approaches are usually not cost-effective and require special purpose hardware.

Given the rapid progress in HPE research, this article attempts to track recent advances and summarize their achievements in order to provide a clear picture of current research on deep learning-based 2D and 3D HPE.

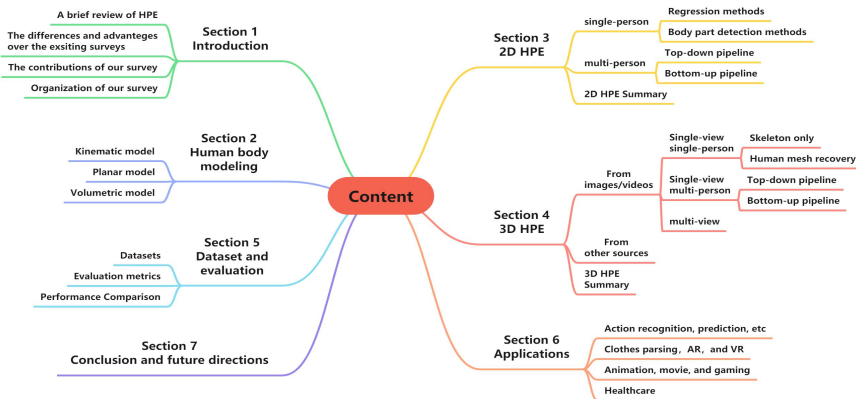


Fig. 1. Taxonomy of this survey.

1.1 Previous surveys and our contributions

There are several related surveys and reviews previously reported on HPE. Among them, [86, 162, 163, 193] focus on the general field of visual-based human motion capture including pose estimation, tracking, and action recognition. Therefore, pose estimation is only one of the topics covered in these surveys. The research works on 3D HPE before 2012 are reviewed in [68]. The body parts parsing-based methods for single-view and multi-view HPE are reported in [142]. These surveys published during 2001-2015 mainly focus on conventional methods without deep learning. A survey on both traditional and deep learning-based methods related to HPE is presented in [61]. However, only a handful of deep learning-based approaches are included. The survey in [213]

covers 3D HPE methods with RGB inputs, while the survey in [168] only reviews 2D HPE methods. Monocular HPE from the classical to recent deep learning-based methods (till 2019, less than 100 papers) is summarized in [29]. However, it only covers 2D HPE and 3D single-view HPE from monocular cameras. 3D multi-view HPE from monocular cameras and 3D HPE from other sensors are ignored. Also, no extensive performance comparisons or in-depth analyses are given, and the discussion on existing challenges and future directions is relatively short.

This survey aims to address the shortcomings of the previous surveys in terms of providing a systematic review of the recent deep learning-based solutions to 2D and 3D HPE but also covering other aspects of HPE including the performance evaluation of (2D and 3D) HPE methods on popular datasets, their applications, and comprehensive discussion. The key points that distinguish this survey from the previous ones are as follows:

- A comprehensive review of recent deep learning-based 2D and 3D HPE methods (up to 2022 with more than 250 papers) is provided by categorizing them according to 2D or 3D scenario, single-view or multi-view, from monocular images/videos or other sources, and learning paradigm.
- Extensive performance evaluation of 2D and 3D HPE methods. We summarize and compare reported performances of promising methods on common datasets based on their categories. The comparison of results provides cues for the strength and weakness of different methods, revealing the research trends and future directions of HPE.
- An overview of a wide range of HPE applications, such as gaming, surveillance, AR/VR, and healthcare.
- An insightful discussion of 2D and 3D HPE is presented in terms of key challenges in HPE pointing to potential future research towards improving performance.

1.2 Paper organization

We first overview the human body modeling techniques in § 2. Then, HPE is divided into two main categories: 2D HPE (§ 3) and 3D HPE (§ 4). Fig. 1 shows the taxonomy of deep learning methods for HPE. According to the number of people, 2D HPE methods are categorized into single-person and multi-person settings. For single-person methods (§ 3.1), there are two categories of deep learning-based methods: regression methods and heatmap-based methods. For multi-person methods (§ 3.2), there are also two types of methods: top-down methods and bottom-up methods.

3D HPE methods are classified according to the input source types: monocular RGB images and videos (§ 4.1), or other sensors (e.g., inertial measurement unit sensors, § 4.2). The majority of these methods use monocular RGB images and videos, and they are further divided into single-view single person (§ 4.1.1); single-view multi-person (§ 4.1.2); and multi-view methods (§ 4.1.3). Multi-view settings are deployed mainly for multi-person pose estimation. Hence, single-person or multi-person is not specified in this category.

Next, depending on the 2D and 3D HPE pipelines, the datasets and evaluation metrics commonly used are summarized followed by a comparison of results of the promising methods (§ 5). In addition, various applications of HPE such as AR/VR are mentioned (§ 6). Finally, the paper ends by an insightful discussion of some promising directions for future research (§ 7).

2 HUMAN BODY MODELING

Human body modeling is an important aspect of HPE to represent keypoints and features extracted from input data. For example, most HPE methods use an N -joints rigid kinematic model. A human body is a sophisticated entity with joints and limbs, and contains body kinematic structure and body shape information. In many methods, a model-based approach is employed to infer and render 2D/3D human body poses. There are typically three types of models for human body modeling, i.e.,

kinematic model (used for 2D/3D HPE), planar model (used for 2D HPE) and volumetric model (used for 3D HPE), as shown in Fig. 2.

Kinematic model. The kinematic model uses a set of joint positions and the limb orientations to represent the human body structure (see Fig. 2 (a)). The pictorial structure model (PSM) [308] is a widely used graph model, which is also known as the tree-structured model. This flexible and intuitive human body model is successfully utilized in 2D HPE [15, 92] and 3D HPE [27, 159]. Although the kinematic model has the advantage of flexible graph-representation, it is limited in representing texture and shape information.

Planar model. Other than the kinematic model to capture the relations between different body parts, the planar model is used to represent the shape and appearance of a human body as shown in Fig. 2 (b). In the planar model, body parts are usually represented by rectangles approximating the human body contours. One example is the cardboard model [96], which is composed of body part rectangular shapes representing the limbs of a person. One of the early works [87] used the cardboard model in HPE. Another example is Active Shape Model (ASM) [44], which is widely used to capture the full human body graph and the silhouette deformations using principal component analysis [58, 236].

Volumetric model. With the increasing interest in 3D human reconstruction, many volumetric human body models (an example representation is depicted in Fig. 2 (c)) have been proposed for a wide variety of human body shapes. The SMPL (Skinned Multi-Person Linear) model [144] is a widely used model in 3D HPE, which can be modeled with natural pose-dependent deformations exhibiting soft-tissue dynamics. To learn how people deform with pose, there are 1786 high-resolution 3D scans of different subjects of poses with template mesh in SMPL to optimize the blend weights [100], pose-dependent blend shapes, the mean template shape, and the regressor from vertices to joint locations. There are also other popular volumetric models such as DYNA [192], Stitched Puppet model [307], Frankenstein & Adam [95], and GHUM & GHUML(ite) [259].

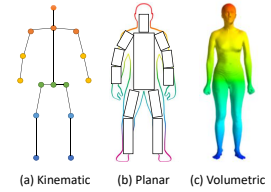


Fig. 2. Models for human body modeling.

3 2D HUMAN POSE ESTIMATION

2D HPE methods estimate the 2D position or spatial location of human body keypoints from images or videos. Traditional 2D HPE methods adopt different hand-crafted feature extraction techniques for body parts, and these early works describe human body as a stick figure to obtain global pose structures. Recently, deep learning-based approaches have achieved a major breakthrough in HPE by improving the performance significantly. In the following, we review deep learning-based 2D HPE methods with respect to single-person and multi-person scenarios.

3.1 2D single-person pose estimation

2D single-person pose estimation is used to localize human body joint positions when the input is a single-person image. If there are more than one person, the input image is cropped first so that there is only one person in each cropped patch (or sub-image). This process can be achieved automatically by an upper-body detector [160] or a full-body detector [203]. In general, there are two categories for single-person pipelines that employ deep learning techniques: regression methods and heatmap-based methods. Regression methods apply an end-to-end framework to learn a mapping from the input image to body joints or parameters of human body models [231]. The goal of heatmap-based methods is to predict approximate locations of body parts and joints [26] [170], which are supervised by heatmaps representation [229, 251]. Heatmap-based frameworks are now widely used in 2D HPE tasks. The general frameworks of 2D single-person HPE methods are depicted in Fig. 3.

3.1.1 Regression methods. There are many works based on the **regression framework** (e.g., [16, 54, 121, 123, 147, 148, 152, 153, 171, 177, 189, 219, 231, 277]) to predict joint coordinates from images as shown in Fig. 3 (a). Using AlexNet [110] as the backbone, Toshev and Szegedy [231] proposed a cascaded deep neural network regressor named DeepPose to learn keypoints from images. Due to the impressive performance of DeepPose, the research paradigm of HPE began to shift from classic approaches to deep learning, in particular convolutional neural networks (CNNs). Based on GoogLeNet [220], Carreira et al. [16] proposed an Iterative Error Feedback (IEF) network, which is a self-correcting model to progressively change an initial solution by injecting the prediction error back to the input space. Sun et al. [219] introduced a structure-aware regression method called "compositional pose regression" based on ResNet-50 [67]. This method adopts a re-parameterized and bone-based representation that contains human body information and pose structure, instead of the traditional joint-based representation. Luvizon et al. [148] proposed an end-to-end regression approach for HPE using softmax function to convert feature maps into joint coordinates in a fully differentiable framework. Li et al. [121] took full advantage of the encoder-decoder architecture from the transformer [238] and designed a cascaded transformer-based model PRTR, which can obtain the spatial relations from the joints for the keypoints prediction with regression inference.

A good feature that encodes rich pose information is critical for regression-based methods. One popular strategy to learn better feature representation is **multi-task learning** [208]. By sharing representations between related tasks (e.g., pose estimation and pose-based action recognition), the model can generalize better on the original task (pose estimation). Following this direction, Li et al. [123] proposed a heterogeneous multi-task framework that consists of two tasks: predicting joints coordinates from full images by a regressor and detecting body parts from image patches using a sliding window. Fan et al. [54] proposed a dual-source (i.e., image patches and full images) CNN for two tasks: joint detection which determines whether a patch contains a body joint, and joint localization which finds the exact location of the joint in the patch. Each task corresponds to a loss function, and the combination of two tasks leads to improved results. Luvizon et al. [147] learned a multi-task network to jointly handle 2D/3D pose estimation and action recognition from videos.

3.1.2 Heatmap-based methods. Heatmap-based methods for HPE aim to train a body part detector to predict the positions of body joints. Detection methods for HPE tackle the estimation task with a heatmap prediction approach. Concretely, the goal is to estimate K heatmaps $\{H_1, H_2, \dots, H_K\}$ for a total of K keypoints. The pixel value $H_i(x, y)$ in each keypoint heatmap indicates the probability that the keypoint lies in the position (x, y) (see Fig. 3 (b)). The target (or ground-truth) heatmap is generated by a 2D Gaussian centered at the ground-truth joint location [229][230]. Thus pose estimation networks are trained by minimizing the discrepancy (e.g., the Mean Squared-Error (MSE)) between the predicted heatmaps and target heatmaps.

Compared with joint coordinates, heatmaps provide richer supervision information by preserving the spatial location information to facilitate the training of convolutional networks. Therefore, there is a recent growing interest in leveraging heatmaps to represent the joint locations and developing **effective CNN architectures** for HPE, e.g., [6, 7, 10, 47, 60, 134, 146, 170, 199, 229,

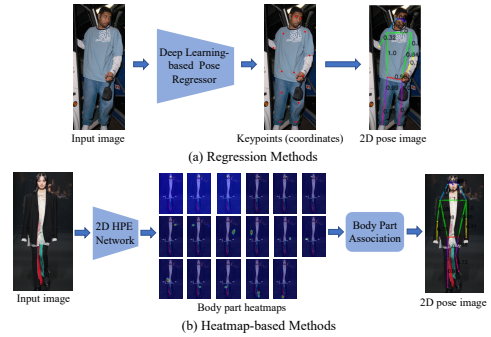


Fig. 3. Single-person 2D HPE frameworks. (a) Regression methods directly learn a mapping (via a deep neural network) from the original image to the kinematic body model and produce joint coordinates. (b) Heatmap-based methods predict body joint locations using the supervision of heatmaps.

230, 251, 256, 265, 278]. Tompson et al. [230] combined CNN-based body part detector with a part-based spatial-model into a unified learning framework for 2D HPE. Lifshitz et al. [134] proposed a CNN-based method for predicting the locations of joints. It incorporates the keypoints votes and joint probabilities to determine the human pose representation. Wei et al. [251] introduced a convolutional networks-based sequential framework named Convolutional Pose Machines (CPM) to predict the locations of key joints with multi-stage processing (the convolutional networks in each stage utilize the 2D belief maps generated from previous stages and produce the increasingly refined predictions of body part locations). Newell et al. [170] proposed an encoder-decoder network named "stacked hourglass" to repeat bottom-up and top-down processing with intermediate supervision. The stacked hourglass (SHG) network consists of consecutive steps of pooling and upsampling layers to capture information at every scale. Since then, complex variations of the SHG architecture were developed for HPE. Chu et al. [41] designed novel Hourglass Residual Units (HRUs), which extend the residual units with a side branch of filters with larger receptive fields, to capture features from various scales. Yang et al. [265] designed a multi-branch Pyramid Residual Module (PRM) to replace the residual unit in SHG, leading to enhanced invariance in scales of deep CNNs.

With the emergence of **Generative Adversarial Networks (GANs)** [62], they are explored in HPE to generate biologically plausible pose configurations and to discriminate the predictions with high confidence from those with low confidence, which could infer the poses of the occluded body parts. Chen et al. [28] constructed a structure-aware conditional adversarial network—Adversarial PoseNet—which contains an hourglass network-based pose generator and two discriminators to discriminate against reasonable body poses from unreasonable ones. Chou et al. [39] built an adversarial learning-based network with two stacked hourglass networks sharing the same structure as discriminator and generator, respectively. The generator estimates the location of each joint, and the discriminator distinguishes the ground-truth heatmaps and predicted ones. Different from GANs-based methods that take HPE network as the generator and utilize the discriminator to provide supervision, Peng et al. [187] developed an adversarial data augmentation network to optimize data augmentation and network training by treating HPE network as a discriminator and using augmentation network as a generator to perform adversarial augmentations.

Besides these efforts in effective network design for HPE, **body structure information** is also investigated to provide more and better supervision information for building HPE networks. Yang et al. [266] designed an end-to-end CNN framework for HPE, which is able to find hard negatives by incorporating the spatial and appearance consistency among human body parts. A structured feature-level learning framework was proposed in [40] for reasoning the correlations among human body joints in HPE, which captures richer information of human body joints and improves the learning results. Ke et al. [101] designed a multi-scale structure-aware neural network, which combines multi-scale supervision, multi-scale feature combination, structure-aware loss information scheme, and a keypoint masking training method to improve HPE models in complex scenarios. Tang et al. [222] built a hourglass-based supervision network, termed as Deeply Learned Compositional Model, to describe the complex and realistic relationships among body parts and learn the compositional pattern information (the orientation, scale and shape information of each body part) in human bodies. Tang and Wu [221] revealed that not all parts are related to each other, therefore introduced a Part-based Branches Network to learn representations specific to each part group rather than a shared representation for all parts.

Human poses in video sequences are (3D) spatio-temporal signals. Therefore, modeling the spatio-temporal information is important for HPE from videos. Jain et al. [82] designed a two-branch CNN framework to incorporate both color and motion features within frame pairs to build an expressive temporal-spatial model in HPE. Pfister et al. [188] proposed a CNN that can utilize temporal context information from multiple frames by using optical flow to align predicted

heatmaps from neighbouring frames. Different from the previous video-based methods which are computationally intensive, Luo et al. [146] introduced a recurrent structure with Long Short-Term Memory to capture temporal geometric consistency and dependency from different frames. This method results in a faster speed in training the HPE network for videos. Zhang et al. [285] introduced a key frame proposal network for capturing spatial and temporal information from frames, and a human pose interpolation module for efficient video-based HPE.

3.2 2D multi-person pose estimation

Compared to single-person HPE, multi-person HPE is more difficult and challenging because it needs to figure out the number of people and their positions, and how to group keypoints for different people. In order to solve these problems, multi-person HPE methods can be classified into top-down and bottom-up methods. Top-down methods employ off-the-shelf person detectors to obtain a set of boxes (each corresponding to one person) from the input images, and then apply single-person pose estimators to each person box to generate multi-person poses. Different from top-down methods, bottom-up methods locate all the body joints in one image first and then group them to the corresponding subjects. In the top-down pipeline, the number of people in the input image will directly affect the computing time. The computing speed for bottom-up methods is usually faster than top-down methods since they do not need to detect the pose for each person separately. Fig. 4 shows the general frameworks for 2D multi-person HPE methods.

3.2.1 Top-down pipeline. In the top-down pipeline as shown in Fig. 4 (a), there are two important parts: a human body detector to obtain person bounding boxes and a single-person pose estimator to predict the locations of keypoints within these bounding boxes. A line of works focus on **designing and improving the modules** in HPE networks, e.g., [13, 71, 72, 127, 165, 179, 218, 245, 256, 276]. To answer the question "how good could a simple method be" in building an HPE network, Xiao et al. [256] added a few deconvolutional layers in the ResNet (backbone network) to build a simple yet effective structure to produce heatmaps for high-resolution representations. Sun et al. [218] presented a novel High-Resolution Net (HRNet) to learn reliable high resolution representations by connecting multi-resolution subnetworks in parallel and conducting repeated multi-scale fusions. To improve the accuracy of keypoint localization, Wang et al. [245] introduced a two-stage graph-based and model-agnostic framework, called Graph-PCNN. It consists of a localization subnet to obtain rough keypoint locations and a graph pose refinement module to get refined keypoints localization representations. Cai et al. [13] introduced a multi-stage network with a Residual Steps Network (RSN) module to learn delicate local representations by efficient intra-level feature fusion strategies, and a Pose Refine Machine (PRM) module to find a trade-off between local and global representations in the features.

Estimating poses under occlusion and truncation scenes often occurs in multi-person settings since the overlapping of limbs is inevitable. Human detectors may fail in the first step of top-down pipeline due to occlusion. Thus, robustness to occlusion or truncation is an important aspect

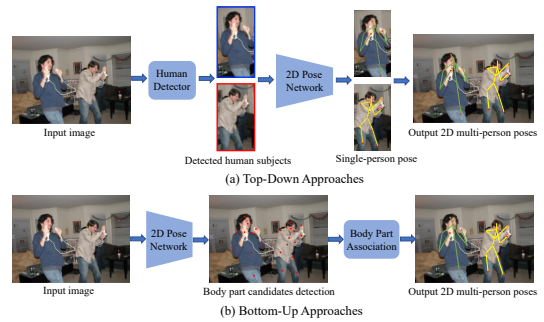


Fig. 4. Illustration of the multi-person 2D HPE frameworks. (a) Top-down approaches have two sub-tasks: (1) human detection and (2) pose estimation in the region of a single human; (b) Bottom-up approaches also have two sub-tasks: (1) detect all keypoints candidates of body parts and (2) associate body parts in different human bodies and assemble them into individual pose representations.

of the multi-person HPE approaches. Towards this goal, Iqbal and Gall [78] built a convolutional pose machine-based pose estimator to estimate the joint candidates. Then they used integer linear programming to solve the joint-to-person association problem and obtain the human body poses even in presence of severe occlusions. Fang et al. [55] designed a regional multi-person pose estimation (RMPE) approach to improve the performance of HPE in complex scenes. The RMPE framework has three parts: Symmetric Spatial Transformer Network (to detect single person region within inaccurate bounding box), Parametric Pose Non-Maximum-Suppression (to solve the redundant detection problem), and Pose-Guided Proposals Generator (to augment training data). Papandreou et al. [179] proposed a two-stage architecture with a Faster R-CNN person detector to create bounding boxes for candidate human bodies and a keypoint estimator to predict the locations of keypoints by using a form of heatmap-offset aggregation. The method works well in occluded and cluttered scenes. To alleviate the occlusion problem in HPE, Chen et al. [30] presented a Cascade Pyramid Network (CPN) which includes two parts: GlobalNet (a feature pyramid network to predict the invisible keypoints) and RefineNet (a network to integrate all levels of features from the GlobalNet with a keypoint mining loss). Their results reveal that CPN has a good performance in predicting occluded keypoints. Su et al. [216] designed two modules, the Channel Shuffle Module and the Spatial & Channel-wise Attention Residual Bottleneck, to achieve channel-wise and spatial information enhancement for better multi-person HPE under occluded scenes. Qiu et al. [198] developed an Occluded Pose Estimation and Correction module and an occluded pose dataset to solve the occlusion problem in crowd pose estimation. Umer et al. [235] proposed a keypoint correspondence framework to recover missed poses using temporal information of the previous frame in occluded scene. The network is trained using self-supervision to improve the pose estimation results on sparsely annotated video datasets.

Recently, the **transformer-based methods** attract more attention [128, 130, 264], since the attention modules in transformer can obtain long-range dependencies and global evidence of the predicted keypoints, which are more powerful than CNNs. The early exploration [264] proposed a transformer-based model for 2D HPE named TransPose, which utilizes the attention layers to predict the heatmaps of the keypoints and learn the fine-grained evidence for HPE in occlusion scenarios. Following [264], Li et al. [130] built a pure transformer-based model named TokenPose to capture the constraint cues and visual appearance relationships by using token representation.

3.2.2 Bottom-up pipeline. The bottom-up pipeline (e.g., [15, 32, 56, 75, 76, 90, 109, 169, 174, 191, 226]) has two main steps including body joint detection (i.e., extracting local features and predicting body joint candidates) and joint candidates assembling for individual bodies (i.e., grouping joint candidates to build pose representations with part association strategies) as shown in Fig. 4 (b).

Pishchulin et al. [191] proposed a Fast R-CNN based body part detector named DeepCut, which is one of the earliest **two-stage** bottom-up approaches. It first detects all the body part candidates, then labels each part and assembles these parts using integer linear programming (ILP) to a final pose. However, DeepCut is computationally expensive. To this end, Insafutdinov et al. [76] introduced DeeperCut to improve DeepCut by applying a stronger body part detector with a better incremental optimization strategy and image-conditioned pairwise terms to group body parts, leading to improved performance as well as a faster speed. Later, Cao et al. [15] built a detector named OpenPose, which uses Convolutional Pose Machines [251] to predict keypoint coordinates via heatmaps and Part Affinity Fields (PAFs, a set of 2D vector fields with vectormaps that encode the position and orientation of limbs) to associate the keypoints to each person. OpenPose largely accelerates the speed of bottom-up multi-person HPE. Based on the OpenPose framework, Zhu et al. [305] improved the OpenPose structure by adding redundant edges to increase the connections between joints in PAFs and obtained better performance than the baseline approach. Although

OpenPose-based methods have achieved impressive results on high resolution images, they have poor performance with low resolution images and occlusions. To address this problem, Kreiss et al. [109] proposed a bottom-up method called PifPaf that uses a Part Intensity Field to predict the locations of body parts and a Part Association Field to represent the joints association. This method outperformed previous OpenPose-based approaches on low resolution and occluded scenes. Motivated by OpenPose [15] and stacked hourglass structure [170], Newell et al. [169] introduced a **single-stage** deep network to simultaneously obtain pose detection and group assignments. Following [169], Jin et al. [90] proposed a new differentiable Hierarchical Graph Grouping method to learn the human part grouping. Based on [169] and [218], Cheng et al. [32] proposed an extension of HRNet, named Higher Resolution Network, which deconvolves the high-resolution heatmaps generated by HRNet to solve the scale variation challenge in bottom-up multi-person HPE.

Multi-task structures are also employed in bottom-up HPE methods. Papandreou et al. [178] introduced PersonLab to combine the pose estimation module and the person segmentation module for keypoints detection and association. PersonLab consists of short-range offsets (for refining heatmaps), mid-range offsets (for predicting the keypoints) and long-range offsets (for grouping keypoints into instances). Kocabas et al. [104] presented a multi-task learning model with a pose residual net, named MultiPoseNet, which can perform keypoints prediction, human detection and semantic segmentation tasks altogether.

3.3 2D HPE Summary

In summary, the performance of 2D HPE has been significantly improved with the blooming of deep learning techniques. In recent years, deeper and more powerful networks have enhanced the performance of 2D single-person HPE methods such as DeepPose [231] and Stacked Hourglass Network [170], as well as in 2D multi-person HPE like AlphaPose [55] and OpenPose [15].

Although promising performance has been achieved, there are several challenges in 2D HPE that need to be further addressed in future research. First is the reliable detection of individuals under significant occlusion [30], e.g., in crowd scenarios. Person detectors in top-down 2D HPE methods may fail to identify the boundaries of largely overlapped human bodies. Similarly, the difficulty of keypoint association is more pronounced for bottom-up approaches in occluded scenes.

The second challenge is computation efficiency. Although some methods like OpenPose [15] can achieve near real-time processing on special hardware with moderate computing power (e.g., 22 FPS on a machine with a Nvidia GTX 1080 Ti GPU), it is still difficult to implement the networks on resource-constrained devices. Real-world applications (e.g., online coaching, gaming, AR and VR) require more efficient HPE methods on commercial devices which can bring better interaction experience for users.

Another challenge lies in the limited data for rare poses. Although the size of current datasets for 2D HPE is large enough (e.g., COCO dataset [137]) for the normal pose estimation (e.g., standing, walking, running), these datasets have limited training data for unusual poses, e.g., falling. The data imbalance may cause model bias, resulting in poor performance on those poses. It would be useful to develop effective data generation or augmentation techniques to generate extra pose data for training more robust models.

4 3D HUMAN POSE ESTIMATION

3D HPE, which aims to predict locations of body joints in 3D space, has attracted much interest in recent years since it can provide extensive 3D structure information related to human body. It can be applied to various applications (e.g., 3D movie and animation industries, virtual reality, and sport analysis). Although significant improvements have been achieved in 2D HPE, 3D HPE still remains as a challenging task. Most existing works tackle 3D HPE from monocular images

or videos, which is an ill-posed and inverse problem due to projection of 3D to 2D where one dimension is lost. When multiple views are available or other sensors such as IMU and LiDAR are deployed, 3D HPE can be a well-posed problem employing information fusion techniques. Another limitation is that deep learning models are data-hungry and sensitive to the data collection environment. Unlike 2D HPE datasets where accurate 2D pose annotation can be easily obtained, collecting accurate 3D pose annotation is time-consuming and manual labeling is not practical. Also, datasets are usually collected from indoor environments with selected daily actions. Recent works [242, 267, 298] revealed the poor generalization of models trained with biased datasets by cross-dataset inference. In this section, we first focus on 3D HPE from monocular RGB images and videos, and then cover 3D HPE based on other sensors.

4.1 3D HPE from monocular RGB images and videos

The monocular camera is the most widely used sensor for HPE in both 2D and 3D scenarios. Recent progress of deep learning-based 2D HPE from monocular images and videos has enabled researchers to extend their works to 3D HPE.

The reconstruction of 3D human poses from a single view of monocular images and videos is a nontrivial task that suffers from self-occlusions and other object occlusions, depth ambiguities, and insufficient training data. It is a severely ill-posed problem because different 3D human poses can be projected to a similar 2D pose projection.

Occlusion problem can be alleviated by estimating 3D human pose from multi-view cameras. In multi-view setting, the viewpoints association need to be addressed. Thus deep learning-based 3D HPE methods are divided into three categories: single-view single person 3D HPE, single-view multi-person 3D HPE, and multi-view 3D HPE.

4.1.1 Single-view single person 3D HPE. Single-person 3D HPE approaches can be classified into skeleton-only and human mesh recovery (HMR) categories based on whether to reconstruct 3D human skeleton or to recovery 3D human mesh by employing a human body model (as listed in Section 2.)

A. Skeleton-only. The skeleton-only methods estimate 3D human joints as the final output. They do not employ human body models to reconstruct 3D human mesh representation. These methods can be further divided into direct estimation approaches and 2D to 3D lifting approaches.

Direct estimation: As shown in Fig. 5(a), direct estimation methods infer the 3D human pose from 2D images without intermediately estimating 2D pose representation, e.g., [124, 182, 183, 219, 223]. Li and Chan [122] employed a shallow network to train the body part detector with sliding windows and the pose coordinate regression synchronously. Sun et al. [219] proposed a structure-aware regression approach. Instead of using joint-based representation, they adopted a bone-based representation with more stability. A compositional loss was defined by exploiting 3D bone structure with bone-based representation that encodes long range interactions between the bones. Pavlakos et al. [182, 183] introduced a volumetric representation to convert the highly non-linear 3D coordinate regression problem to a manageable form in a discretized space. The voxel likelihoods for each joint in the volume were predicted by a convolutional network. Ordinal depth relations of human joints were used to alleviate the need for accurate 3D ground truth pose.

2D to 3D lifting: Motivated by the recent success of 2D HPE, 2D to 3D lifting approaches that infer 3D human pose from the intermediately estimated 2D human pose have become a popular 3D HPE solution as illustrated in Fig. 5 (b). In the first stage, off-the-shelf 2D HPE models are employed to estimate 2D pose. Then 2D to 3D lifting is used to obtain 3D pose in the second stage, e.g., [17, 117, 155, 167, 224, 297]. Benefiting from the excellent performance of state-of-the-art 2D pose detectors, 2D to 3D lifting approaches generally outperform direct estimation approaches. Martinez

et al. [155] proposed a fully connected residual network to regress 3D joint locations based on the 2D joint locations. Despite achieving the state-of-the-art results at that time, the method could fail due to reconstruction ambiguity of over-reliance on the 2D pose detector. Tekin et al. [224] and Zhou et al. [297] adopted 2D heatmaps instead of 2D pose as intermediate representations for estimating 3D pose. Wang et al. [249] developed a pairwise ranking CNN to predict the depth ranking of pairwise human joints. Then, a coarse-to-fine pose estimator was used to regress the 3D pose from 2D joints and the depth ranking matrix. Jahangiri and Yuille [81], Sharma et al. [214], and Li and Lee [117] first generated multiple diverse 3D pose hypotheses then applied ranking networks to select the best 3D pose.

Given that a human pose can be represented as a graph where the joints are the nodes and the bones are the edges, **Graph Convolutional Networks (GCNs)** have been applied to the 2D-to-3D pose lifting problem by showing promising performance [38, 42, 140, 274, 288]. Ci et al. [42] proposed a Locally Connected Network (LCN), which leverages both fully connected network and GCN to encode the relationship between local joint neighborhoods. LCN can overcome the limitations of GCN that weight sharing scheme harms pose estimation model's representation ability, and the structure matrix lacks flexibility to support customized node dependence. Zhao et al. [288] also tackled the limitation of the shared weight matrix of convolution filters for all the nodes in GCN. A Semantic-GCN was proposed to investigate the semantic information and relationship.

The semantic graph convolution (SemGConv) operation is used to learn channel-wise weights for edges. Both local and global relationships among nodes are captured since SemGConv and non-local layers are interleaved. Zhou et al. [306] further introduced a novel modulated GCN network which consists of weight modulation and affinity modulation. The weight modulation exploits different modulation vectors for different nodes that let the feature transformations be disentangled. The affinity modulation explores additional joint correlations beyond the defined human skeleton.

The kinematic model is an articulated body representation by connected bones and joints with kinematic constraints, which has gained increasing attention in 3D HPE in recent years. Many methods leverage prior knowledge based on the kinematic model such as skeletal joints connectivity information, joints rotation properties, and fixed bone-length ratios for plausible pose estimation, e.g., [59, 114, 159, 172, 173, 244, 260, 299]. Zhou et al. [299] embedded a kinematic model into a network as kinematic layers to enforce the orientation and rotation constraints. Nie et al. [172] and Lee et al. [116] employed a skeleton-LSTM network to leverage joint relations and connectivity. Observing that human body parts have a distinct degree of freedom (DOF) based on the kinematic structure, Wang et al. [244] and Nie et al. [173] proposed bidirectional networks to model the kinematic and geometric dependencies of the human skeleton. Kundu et al. [114] [113] designed a kinematic structure preservation approach by inferring local-kinematic parameters with energy-based loss and explored 2D part segments based on the parent-relative local limb kinematic model. Xu et al. [260] demonstrated that noisy 2D joint is one of the key obstacles for accurate 3D pose estimation. Hence a 2D pose correction module was employed to refine unreliable 2D joints

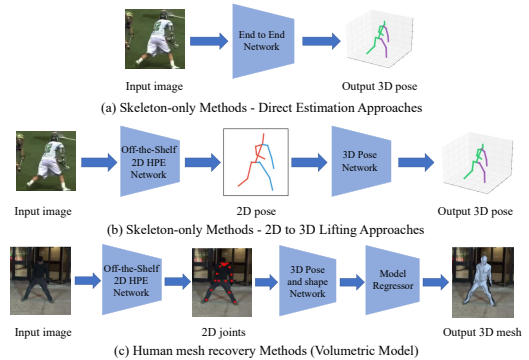


Fig. 5. Single-person 3D HPE frameworks. (a) Direct estimation approaches directly estimate the 3D human pose from 2D images. (b) 2D to 3D lifting approaches leverage the predicted 2D human pose (intermediate representation) for 3D pose estimation. (c) Human mesh recovery methods incorporate parametric body models to recover high-quality 3D human mesh. The 3D pose and shape parameters inferred by the 3D pose and shape network are fed into the model regressor to reconstruct 3D human mesh. Part of the figure is from [5].

based on the kinematic structure. Zanfir et al. [271] introduced a kinematic latent normalizing flow representation (a sequence of invertible transformations applied to the original distribution) with differentiable semantic body part alignment loss functions.

3D HPE datasets are usually collected from controlled environments with selected daily motions. It is difficult to obtain accurate 3D pose annotations for in-the-wild data. Thus 3D HPE for **in-the-wild data with unusual poses and occlusions** is still a challenge. To this end, a group of 2D to 3D lifting methods pay attention to estimate the 3D human pose from in-the-wild images without 3D pose annotations such as [18, 65, 242, 267, 298]. Zhou et al. [298] proposed a weakly supervised transfer learning method that uses 2D annotations of in-the-wild images as weak labels. 3D pose estimation module was connected with intermediate layers of the 2D pose estimation module. For in-the-wild images, 2D pose estimation module performed a supervised 2D heatmap regression and a 3D bone length constraint induced loss was applied in the weakly supervised 3D pose estimation module. Habibie et al. [65] tailored a projection loss to refine the 3D human pose without 3D annotation. A 3D-2D projection module was designed to estimate the 2D body joint locations with the predicted 3D pose from earlier network layer. The projection loss was used to update the 3D human pose without requiring 3D annotations. Inspired by [50], Chen et al. [18] proposed an unsupervised lifting network based on the closure and invariance lifting properties with a geometric self-consistency loss for the lift-reproject-lift process. Closure means for a lifted 3D skeleton, after random rotation and re-projection, the resulting 2D skeleton will lie within the distribution of valid 2D pose. Invariance means when changing the viewpoint of 2D projection from a 3D skeleton, the re-lifted 3D skeleton should be the same.

Instead of estimating 3D human pose from monocular images, **videos can provide temporal information** to improve accuracy and robustness of 3D HPE, e.g., [12, 35, 45, 186, 225, 247, 301, 302]. Hossain and Little [200] proposed a recurrent neural network using a Long Short-Term Memory (LSTM) unit with shortcut connections to exploit temporal information from sequences of human pose. Their method exploits the past events in a sequence-to-sequence network to predict temporally consistent 3D pose. Noticing that the complementary property between spatial constraints and temporal correlations is usually ignored by prior work, Dabral et al. [45], Cai et al. [12], and Li et al. [132] exploited the spatial-temporal relationships and constraints (e.g., bone-length constraint and left-right symmetry constraint) to improve 3D HPE performance from sequential frames. Pavllo et al. [186] proposed a temporal convolution network to estimate 3D pose over 2D keypoints from consecutive 2D sequences. However, their method is based on the assumption that prediction errors are temporally non-continuous and independent, which may not hold in presence of occlusions [35]. Based on [186], Chen et al. [22] added bone direction module and bone length module to ensure human anatomy temporal consistency across video frames, while Liu et al. [141] utilized the attention mechanism to recognize significant frames and model long-range dependencies in large temporal receptive fields. Zeng et al. [274] employed the split-and-recombine strategy to address the rare and unseen pose problem. The human body is first split into local regions for processing through separate temporal convolutional network branches, then the low-dimensional global context obtained from each branch is combined to maintain global coherence.

Transformer architectures have become the model of choice in natural language processing and now is developing rapidly in the field of computer vision. Recent works have demonstrated the powerful global representation ability of transformer attention mechanism in various vision tasks [102]. Zheng et al. [294] presented the first purely transformer-based approach for 3D HPE without convolutional architectures involved. The spatial transformer module encodes local relationships between human body joints, and the temporal transformer module captures the global dependencies across frames in the entire sequence. Li et al. [125] proposed a strided transformer encoder (STE) to reduce the sequence redundancy and computation cost. The long-range information of pose

sequences was aggregated to a single vector representation containing local and global correlations in a hierarchical architecture. Li et al. [126] further designed a multi-hypothesis transformer to exploit spatial-temporal representations of multiple pose hypotheses. Zhao et al. [291] integrated transformer architecture with graph convolution to capture human kinematic structured and implicit joint relations using much fewer parameters.

B. Human Mesh Recovery (HMR). HMR methods incorporate parametric body models as noted in Section 2 to recovery human mesh as shown in Fig. 5(c). The 3D pose can be obtained by using the model-defined joint regression matrix [106].

Volumetric models are used to recover high-quality human mesh, providing extra shape information of human body. As one of the most popular volumetric models, the SMPL model [144] has been widely used in 3D HPE, e.g., [5, 9, 89, 106, 111, 120, 166, 262, 280, 281, 303], because it is compatible with existing rendering engines. Tan et al. [239], Tung et al. [234], Pavlakos et al. [185], and Omran et al. [175] regressed SMPL parameters to reconstruct 3D human mesh. Instead of predicting SMPL parameters, Kolotouros et al. [107] regressed the locations of the SMPL mesh vertices using a Graph-CNN architecture. Kocabas et al. [103] included the large-scale motion capture dataset AMASS [151] for adversarial training of their SMPL-based method named VIBE (Video Inference for Body Pose and Shape Estimation). VIBE leveraged AMASS to discriminate between real human motions and predicted pose by pose regression module. Since low-resolution visual content is more common in real-world scenarios than the high-resolution visual content, existing well-trained models may fail when resolution is degraded. Xu et al. [262] introduced the contrastive learning scheme into self-supervised resolution-aware SMPL-based network. The self-supervised contrastive learning scheme uses a self-supervision loss and a contrastive feature loss to enforce the feature and scale consistency. Choi et al. [37] presented a temporally consistent mesh recovery system (named TCMR) to produce temporally consistent and smooth 3D human motion output from a video. Kolotouros et al. [108] proposed a probabilistic model using conditional normalizing flow for 3D human mesh recovery from 2D evidence.

There are a few recent attempts to utilize transformer architecture in HMR. Lin et al. proposed METRO [135] and MeshGraphormer [136] that combine CNNs with transformer networks to regress SMPL mesh vertices from a single image. However, METRO and MeshGraphormer pursued higher accuracy while sacrificing computation and memory. Zheng et al. [293] designed a lightweight transformer-based method that can reconstruct human mesh from 2D human pose with a significant computation and memory cost reduction.

There are several **extended SMPL-based models** to address the limitations of the SMPL model such as high computational complexity, and lack of hands and facial landmarks. SMPLify [9, 115] is an optimization method which fits the SMPL model to the detected 2D joints and minimizes the re-projection error. Pavlakos et al. [181] introduced a new model, named SMPL-X, that can also predict fully articulated hands and facial landmarks. Following the SMPLify method, they also proposed SMPLify-X, which is an improved version learned from AMASS dataset [151]. Hassan et al. [66] further extended SMPLify-X to PROX – a method enforcing Proximal Relationships with Object eXclusion by adding 3D environmental constraints. Kolotouros et al. [106] integrated the regression-based and optimization-based SMPL parameter estimation methods to a new one named SPIN (SMPL oPtimization IN the loop) while employing SMPLify in the training loop. Osman et al. [176] upgraded SMPL to STAR by training with additional 10,000 scans for better model generalization. The number of model parameters is reduced to 20% of that of SMPL.

Instead of using the SMPL-based model, other models have also been used for recovering 3D human pose or mesh, e.g., [194, 211, 243]. Chen et al. [36] introduced a Cylinder Man Model to generate occlusion labels for 3D data and performed data augmentation. A pose regularization term was introduced to penalize wrong estimated occlusion labels. Xiang et al. [255] utilized the Adam

model [95] to reconstruct the 3D motions. A 3D human representation, named 3D Part Orientation Fields (POFs), was introduced to encode the 3D orientation of human body parts in the 2D space. Wang et al. [243] presented a new Bone-level Skinned Model of human mesh, which decouples bone modelling and identity-specific variations by setting bone lengths and joint angles. Fisch and Clark [57] introduced an orientation keypoints model which can compute full 3-axis joint rotations including yaw, pitch, and roll for 6D HPE.

4.1.2 Single-view multi-person 3D HPE. For 3D multi-person HPE from monocular RGB images or videos, similar categories as 2D multi-person HPE are noted here: top-down approaches and bottom-up approaches as shown in Fig. 6 (a) and Fig. 6 (b), respectively. The comparison between 2D top-down and bottom-up approaches in Section 3.2 is applicable for the 3D case.

Top-down approaches. Top-down approaches of 3D multi-person HPE first perform human detection to detect each individual person. Then for each detected person, absolute root (center joint of the human) coordinate and 3D root-relative pose are estimated by 3D pose networks. Based on the absolute root coordinate of each person and their root-relative pose, all poses are aligned to the world coordinate. Rogez et al. [206] localized candidate regions of each person to generate potential poses, and used a regressor to jointly refine the pose proposals. This localization-classification-regression method, named LCR-Net, performed well on the controlled environment datasets but could not generalize well to in-the-wild images.

To address this issue, Rogez et al. [207] proposed LCR-Net++ by using synthetic data augmentation for the training data to improve performance. Zanfir et al. [272] added semantic segmentation to the 3D multi-person HPE module with scene constraints. Additionally, the 3D temporal assignment problem was tackled by the Hungarian matching method for video-based multi-person 3D HPE. Moon et al. [164] introduced a camera distance-aware approach that the cropped human images were fed into their developed RootNet to estimate the camera-centered coordinates of human body's roots. Then the root-relative 3D pose of each cropped human was estimated by the proposed PoseNet. Benzine et al. [8] proposed a single-shot approach named PandaNet (Pose estimAtION and Detection Anchor-based Network). A low-resolution anchor-based representation was introduced to avoid the occlusion problem. A pose-aware anchor selection module was developed to address the overlapping problem by removing the ambiguous anchors. An automatic weighting of losses associated with different scales was used to handle the imbalance issue of different sizes of people. Li et al. [118] tackled the lack of global information in the top-down approaches. They adopted a Hierarchical Multi-person Ordinal Relations method to leverage body level semantic and global consistency for encoding the interaction information hierarchically.

Bottom-up approaches. In contrast to the top-down approaches, bottom-up approaches first produce all body joint locations and depth maps, then associate body parts to each person according to the root depth and part relative depth. A key challenge of bottom-up approaches is how to group human body joints belonging to each person. Zanfir et al. [273] formulated the person grouping problem as a binary integer programming (BIP) problem. A limb scoring module was used to estimate candidate kinematic connections of detected joints and a skeleton grouping

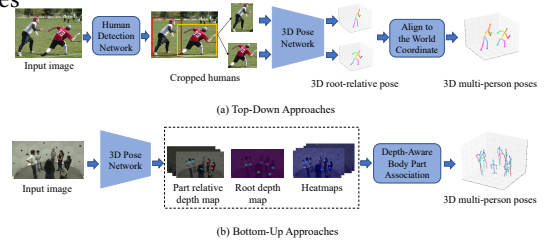


Fig. 6. Illustration of the multi-person 3D HPE frameworks. (a) Top-Down methods first detect single-person regions by human detection network. For each single-person region, individual 3D pose can be estimated by 3D pose network. Then all 3D poses are aligned to the world coordinate. (b) Bottom-Up methods first estimate all body joints and depth maps, then associate body parts to each person according to the root depth and part relative depth. Part of the figure is from [292].

module assembled limbs into skeletons by solving the BIP problem. Nie et al. [174] proposed a Single-stage multi-person Pose Machine (SPM) to define the unique identity root joint for each person. The body joints were aligned to each root joint by using the dense displacement maps. However, this method is limited in that only paired 2D images and 3D pose annotations could be used for supervised learning. Without paired 2D images and 3D pose annotations, Kundu et al. [112] proposed a frozen network to exploit the shared latent space between two diverse modalities under a practical deployment paradigm such that the learning could be cast as a cross-model alignment problem. Fabbri et al. [53] developed a distance-based heuristic for linking joints in a multi-person setting. Specifically, starting from detected heads (i.e., the joint with the highest confidence), the remaining joints are connected by selecting the closest ones in terms of 3D Euclidean distance. Chen et al. [34] integrated top-down and bottom-up approaches in their method. A top-down network first estimates joint heatmaps inside each bounding box, then a bottom-up network incorporates estimated joint heatmaps to handle the scale variation.

Another challenge of bottom-up approaches is occlusion. To cope with this challenge, Metha et al. [158] developed an Occlusion-Robust Pose-Maps (ORPM) approach to incorporate redundancy into the location-maps formulation, which facilitates person association in the heatmaps especially for occluded scenes. Zhen et al. [292] leveraged a depth-aware part association algorithm to assign joints to individuals by reasoning about inter-person occlusion and bone-length constraints. Mehta et al. [157] quickly inferred intermediate 3D pose of visible body joints regardless of the accuracy. Then the completed 3D pose is reconstructed by inferring occluded joints using learned pose priors and global context. The final 3D pose was refined by applying temporal coherence and fitting the kinematic skeletal model.

Comparison of top-down and bottom-up approaches. Top-down approaches usually achieve promising results by relying on the state-of-the-art person detection methods and single-person HPE methods. But the computational complexity and the inference time may become excessive with the increase in the number of humans, especially in crowded scenes. Moreover, since top-down approaches first detect the bounding box for each person, global information in the scene may get neglected. The estimated depth of cropped region may be inconsistent with the actual depth ordering and the predicted human bodies may be placed in overlapping positions. On the contrary, the bottom-up approaches enjoy linear computation and time complexity. However, if the goal is to recover 3D body mesh, it is not straightforward for the bottom-up approaches to reconstruct human body meshes. For top-down approaches, after detecting each individual person, human body mesh of each person can be easily recovered by incorporating the 3D single-person human mesh recovery method. While for the bottom-up approaches, additional model regressor module is needed to reconstruct human body meshes based on the final 3D poses.

4.1.3 Multi-view 3D HPE. The partial occlusion is a challenging problem for 3D HPE in the single-view setting. The natural solution to overcome this problem is to estimate 3D human pose from multiple views, since the occluded part in one view may become visible in other views. In order to reconstruct the 3D pose from multiple views, the association of corresponding location between different cameras needs to be resolved. We do not specify single-person or multi-person in this category since multi-view setting are deployed mainly for multi-person pose estimation.

A group of methods [48, 49, 133, 197, 233] used body models to tackle the association problem by optimizing model parameters to match the model projection with the 2D pose. The widely used 3D pictorial structure model [11] is such a model. However, these methods usually need large memory and expensive computational cost, especially for multi-person 3D HPE under multi-view settings. Rhodin et al. [205] employed a multi-view consistency constraint in the network, however it requires a large amount of 3D ground-truth training data. To overcome this limitation, Rhodin et

al. [204] further proposed an encoder-decoder framework to learn the geometry-aware 3D latent representation from multi-view images and background segmentation without 3D annotations. Chen et al. [25], Dong et al. [48], Chen et al. [19], Mitra et al. [161], Iqbal et al. [79], Zhang et al. [284], and Huang et al. [69] proposed multi-view matching frameworks to reconstruct 3D human pose across all viewpoints with consistency constraints. Pavlakos et al. [184] and Zhang et al. [287] aggregated the 2D keypoint heatmaps of multi-view images into a 3D pictorial structure model based on all the calibrated camera parameters. However, when multi-view camera environments change, the model needs to be retrained. Liang et al. [133] and Habermann et al. [64] inferred the non-rigid 3D deformation parameters to reconstruct a 3D human body mesh from multi-view images. Kadkhodamohammadi and Padoy [98], Qiu et al. [197], and Kocabas et al. [105] employed epipolar geometry to match paired multi-view poses for 3D pose reconstruction and generalized their methods to new multi-view camera environments. It should be noted that matching each pair of views separately without the cycle consistency constraint may lead to incorrect 3D pose reconstructions [48]. Tu et al. [233] aggregated all the features in each camera view in the 3D voxel space to avoid incorrect estimation in each camera view. A cuboid proposal network and a pose regression network were designed to localize all people and to estimate the 3D pose, respectively. When given sufficient viewpoints (more than ten), it is not practical to use all viewpoints for 3D pose estimation. Pirinen et al. [190] proposed a self-supervised reinforcement learning approach to select a small set of viewpoints to reconstruct the 3D pose via triangulation. Wang et al. [250] introduced a transformer-based model that directly regresses 3D poses from multi-view images without relying on any intermediate task. The proposed Multi-view Pose transformer (MvP) was designed to represent query embedding of multi-person joints. The multi-view information was fused by a novel geometrically guided attention mechanism.

Besides accuracy, **the lightweight architecture, fast inference time, and efficient adaptation** to new camera settings also need to be taken into consideration in multi-view HPE. In contrast to [48] which matched all view inputs together, Chen et al. [21] applied an iterative processing strategy to match 2D poses of each view with the 3D pose while the 3D pose was updated iteratively. Compared to the previous methods whose running time may explode with the increase in the number of cameras, their method has linear time complexity. Remelli et al. [202] encoded images of each view into a unified latent representation so that the feature maps were disentangled from camera viewpoints. As a lightweight canonical fusion, these 2D representations are lifted to the 3D pose using a GPU-based Direct Linear Transform to accelerate the processing. In order to improve the generalization ability of the multi-view fusion scheme, Xie et al. [257] proposed a pre-trained multi-view fusion model (MetaFuse), which can be efficiently adapted to new camera settings with few labeled data. They deployed the model-agnostic meta-learning framework to learn the optimal initialization of the generic fusion model for adaptation.

4.2 3D HPE from other sources

Although monocular RGB camera is the most common device used for 3D HPE, other sensors (e.g., depth sensor, IMUs, and radio frequency device) are also used for this purpose.

Depth and point cloud sensors: Depth sensors have gained more attention recently for 3D computer vision tasks due to their low-cost and increased utilization. As one of the key challenges in 3D HPE, the depth ambiguity problem can be alleviated by using depth sensors. Yu et al. [269], Xiong et al. [258], Kadkhodamohammadi et al. [97], and Zhi et al. [295] utilized depth images to estimate 3D human pose.

Compared with depth images, point clouds can provide more information. The state-of-the-art point cloud feature extraction techniques, PointNet [195] and PointNet++ [196], have demonstrated

excellent performance for classification and segmentation tasks. Jiang et al. [88] and Wang et al. [248] combined PointNet++ with the human body model to recover 3D human mesh.

IMUs with monocular images: Wearable Inertial Measurement Units (IMUs) can track the orientation and acceleration of human body parts by recording motions without object occlusions and clothes obstructions. Marcard et al. [240, 241], Huang et al. [74], Zhang et al. [286], and Huang et al. [70] proposed IMU-based HPE methods to reconstruct 3D human pose. However, the drifting problem may occur overtime when using IMUs.

Radio frequency device: Radio frequency (RF) based sensing technology has also been used for 3D HPE, e.g., [290] and [289]. The ability to traverse walls and to bounce off human bodies in the WiFi range without carrying wireless transmitters is the major advantage for deploying a RF-based sensing system. Also, privacy can be preserved due to non-visual data. However, RF signals have a relatively low spatial resolution compared to visual camera images and the RF systems have shown to generate coarse 3D pose estimation.

Other sensors/sources: Besides using the aforementioned sensors, Isogawa et al. [80] estimated 3D human pose from the 3D spatio-temporal histogram of photons captured by a non-line-of-sight (NLOS) imaging system. Some methods [227, 228, 261] tackled the egocentric 3D pose estimation via a fish-eye camera. Saini et al. [209] estimated human motion using images captured by multiple Autonomous Micro Aerial Vehicles (MAVs). Clever et al. [43] focused on the HPE of the rest position in bed from pressure images which were collected by a pressure sensing mat.

4.3 3D HPE Summary

3D HPE has made significant advancements in recent years. Since a large number of 3D HPE methods apply the 2D to 3D lifting strategy, the performance of 3D HPE has been improved considerably due to the progress made in 2D HPE. Some 2D HPE methods such as OpenPose [15], AlphaPose [55], and HRNet [218] have been extensively used as 2D pose detector in 3D HPE methods. Besides the 3D pose, some methods also recover 3D human mesh from images or videos, e.g., [103, 106, 275, 296]. However, despite the progress made so far, there are still several challenges.

One challenge is the model generalization. High-quality 3D ground truth pose annotations depend on motion capture systems which cannot be easily deployed in random environment. Therefore, the existing datasets are mainly captured in constrained scenes. The state-of-the-art methods can achieve promising results on these datasets, but their performance degrades when applied to in-the-wild data. It is possible to leverage gaming engines to generate synthetic datasets with diverse poses and complex scenes, e.g., SURREAL dataset [237] and GTA-IM dataset [14]. However, learning from synthetic data may not achieve the desired performance due to a gap between synthetic and real data distributions.

Same as 2D HPE, robustness to occlusion and computation efficiency are two key challenges for 3D HPE as well. The performance of current 3D HPE methods drops considerably in crowded scenarios due to severe mutual occlusion and possibly low resolution content of each person. 3D HPE is more computation demanding than 2D HPE. For example, 2D to 3D lifting approaches rely on 2D poses as intermediate representations for inferring 3D poses. It is critical to develop computationally efficient 2D HPE pipelines while maintaining high accuracy for pose estimation.

5 DATASETS AND EVALUATION METRICS

Datasets are very much needed in conducting HPE. They are also necessary to provide a fair comparison among different algorithms. In this section, we present the most widely used datasets and evaluation metrics for evaluating 2D and 3D deep learning-based HPE methods. The results achieved by existing methods on these popular datasets are summarized.

Table 1. Datasets for 2D HPE.

Image-based datasets							
Name	Year	Single-Person /Multi-Person	Joints	Number of images			Evaluation protocol
				Train	Val	Test	
LSP [92]	2010	Single	14	1k	-	1k	PCP
LSP-extended [93]	2011	Single	14	10k	-	-	PCP
FLIC [212]	2013	Single	10	5k	-	1k	PCP&PCK
FLIC-full [212]	2013	Single	10	20k	-	-	PCP&PCK
FLIC-plus [230]	2014	Single	10	17k	-	-	PCP&PCK
MPII [3]	2014	Single	16	29k	-	12k	PCPm/PCKh mAp
		Multiple	16	3.8k	-	1.7k	
COCO2016 [137]	2016	Multiple	17	45k	22k	80k	AP
COCO2017 [137]	2017	Multiple	17	64k	2.7k	40k	AP
AIC-HKD [254]	2017	Multiple	14	210k	30k	60k	AP
CrowdPose [119]	2019	Multiple	14	10k	2k	8k	mAP
Video-based datasets							
Name	Year	Single-Person /Multi-Person	Joints	Number of videos			Evaluation protocol
				Train	Val	Test	
Penn Action [283]	2013	Single	13	1k	-	1k	-
J-HMDB [84]	2013	Single	15	0.6k	-	0.3k	-
PoseTrack [2]	2017	Multiple	15	292	50	208	mAP

5.1 Datasets for 2D HPE

Although there are several datasets used for 2D HPE tasks before 2014, only a few recent works use these datasets because they have several shortcomings such as lack of diverse object movements and limited data. Since deep learning-based approaches are fueled by the large amount of training data, this section mainly discusses the recent popular and large-scale 2D human pose datasets.

Max Planck Institute for Informatics (MPII) Human Pose Dataset [3] is a popular dataset for evaluation of articulated HPE. The dataset includes around 25,000 images containing over 40,000 individuals with annotated body joints. The images were systematically collected by a two-level hierarchical method to capture everyday human activities. The entire dataset covers 410 human activities and all the images are labeled. Each image was extracted from a YouTube video and provided with preceding and following un-annotated frames. Moreover, rich annotations including body part occlusions, 3D torso and head orientations are labeled by workers on Amazon Mechanical Turk. Images in MPII are suitable for 2D single-person or multi-person HPE.

Microsoft Common Objects in Context (COCO) Dataset [137] is the most widely used large-scale dataset. It has more than 330,000 images and 200,000 labeled subjects with keypoints, and each individual person is labeled with 17 joints. There are two versions of the COCO datasets for HPE: COCO keypoints 2016 and COCO keypoints 2017. Their difference lies in the training, validation and test split. In addition, Jin et al. [91] proposed COCO-WholeBody Dataset with whole-body annotations for HPE.

We refer the readers to the original references for details about other datasets including **LSP** [92], **FLIC** [212], **AIC-HKD** [254], **CrowdPose** [119], **Penn Action** [283], **J-HMDB** [84], and **PoseTrack** [2]. A summary of these datasets is presented in Table 1.

5.2 Evaluation Metrics for 2D HPE

It is difficult to precisely evaluate the performance of HPE because there are many features and requirements that need to be considered (e.g., upper/full human body, single/multiple pose estimation, the size of human body). As a result, many evaluation metrics have been used for 2D HPE. Here we summarize the commonly used ones.

Percentage of Correct Parts (PCP) [51] is a measure commonly used in early works on 2D HPE, which evaluates stick predictions to report the localization accuracy for limbs. The localization of limbs is determined when the distance between the predicted joint and ground truth joint is less than a fraction of the limb length (between 0.1 to 0.5). In some works, the PCP measure is also referred to as PCP@0.5, where the threshold is 0.5. This measure is used for single-person HPE evaluation. However, PCP has not been widely implemented in latest works because it penalizes

the limbs with short length which are hard to detect. The performance of a model is considered better when it has a higher PCP measure. In order to address the drawbacks of PCP, Percentage of Detected Joints (PDJ) is introduced, where a predicted joint is considered as detected if the distance between predicted joints and true joints is within a certain fraction of the torso diameter[231].

Percentage of Correct Keypoints (PCK) [268] is also used to measure the accuracy of localization of different keypoints within a given threshold. The threshold is set to 50 percent of the head segment length of each test image and it is denoted as PCKh@0.5. PCK is referred to as PCK@0.2 when the distance between detected joints and true joints is less than 0.2 times the torso diameter. The higher the PCK value, the better model performance is regarded.

Average Precision (AP) and Average Recall (AR). AP measure is an index to measure the accuracy of keypoints detection according to precision (the ratio of true positive results to the total positive results) and recall (the ratio of true positive results to the total number of ground truth positives). AP computes the average precision value for recall over 0 to 1. AP has several similar variants. For example, Average Precision of Keypoints (APK) is introduced in [268]. Mean Average Precision (mAP), which is the mean of average precision over all classes, is a widely used metric on the MPII and PoseTrack datasets. Average Recall (AR) is another metric used in the COCO keypoint evaluation [1]. Object Keypoint Similarity (OKS) plays the similar role as the Intersection over Union (IoU) in object detection and is used for AP or AR. This measure is computed from the scale of the subject and the distance between predicted points and ground truth points. The COCO evaluation usually uses mAP across 10 OKS thresholds as the evaluation metric.

Table 2. Comparison of different methods on the MPII dataset for 2D single-person HPE using PCKh@0.5 measure (i.e., the threshold is equal to 50 percent of the head segment length of each test image). **H**: Heatmap; **R**: Regression

Max Planck Institute for Informatics (MPII)										
	Year	Method	Head	Shoulder	Elbow	Wrist	Hip	Knee	Ankle	Mean
H	2016	[76]	96.8	95.2	89.3	84.4	88.4	83.4	78.0	88.5
	2016	[251]	97.8	95.0	88.7	84.0	88.4	82.8	79.4	88.5
	2016	[170]	98.2	96.3	91.2	87.1	90.1	87.4	83.6	90.9
	2017	[41]	98.5	96.3	91.9	88.1	90.6	88.0	85.0	91.5
	2017	[265]	98.5	96.7	92.5	88.7	91.1	88.6	86.0	92.0
	2018	[101]	98.5	96.8	92.7	88.4	90.6	89.3	86.3	92.1
	2018	[222]	98.4	96.9	92.6	88.7	91.8	89.4	86.2	92.3
	2018	[256]	98.5	96.6	91.9	87.6	91.1	88.1	84.1	91.5
	2019	[218]	98.6	96.9	92.8	89.0	91.5	89.0	85.7	92.3
	2019	[278]	98.6	97.0	92.8	88.8	91.7	89.8	86.6	92.5
	2019	[127]	98.4	97.1	93.2	89.2	92.0	90.1	85.5	92.6
	2020	[6]	-	-	-	-	-	-	-	92.7
	2020	[13]	98.5	97.3	93.9	89.9	92.0	90.6	86.8	93.0
	2021	[130]	97.1	95.9	90.4	86.0	89.3	87.1	82.5	90.2
	R	2017	[206]	-	-	-	-	-	-	-
2016		[16]	95.7	91.7	81.7	72.4	82.8	73.2	66.4	81.3
2017		[219]	97.5	94.3	87.0	81.2	86.5	78.5	75.4	86.4
2019		[277]	98.3	96.4	91.5	87.4	90.0	87.1	83.7	91.1
2019		[148]	98.1	96.6	92.0	87.5	90.6	88	82.7	91.2
2021		[121]	97.3	96.0	90.6	84.5	89.7	85.5	79.0	89.5
2021		[152]	98.0	95.9	91.0	86.0	89.8	86.6	82.6	90.4
2022		[153]	-	-	-	-	-	-	-	90.5

Note: [76], [218], [127], [13], [206],[130] are 2D multi-person HPE methods, which are also applied to the single-person case here.

5.3 Performance Comparison of 2D HPE Methods

Single-person 2D HPE: Table 2 shows the comparison results for different 2D single-person HPE methods on the MPII dataset using PCKh@0.5 measure. Although both heatmap-based and regression-based methods have impressive results, they have their own limitations in 2D single-person HPE. Regression methods can learn a nonlinear mapping from input images to keypoint coordinates with an end-to-end framework, which offers a fast learning paradigm and a sub-pixel level prediction accuracy. However, they usually give sub-optimal solutions [148] due to the highly nonlinear problem. Heatmap-based methods outperform regression-based approaches and are more widely used in 2D HPE[127][13][148] since (1) the probabilistic prediction of each pixel in a heatmap can improve the accuracy of locating the keypoints; and (2) heatmaps provide richer supervision information by preserving the spatial location information. However, the precision of

Table 3. Comparison of different 2D multi-person HPE methods on the test-dev set of the COCO dataset using AP measure (AP.5: AP at OKS = 0.50; AP.75: AP at OKS = 0.75; AP(M) is used for medium objects; AP(L) is used for large objects). **Extra**: extra data is used for training. **T**: Top-down; **B**: Bottom-up

Microsoft Common Objects in Context (COCO)										
	Year	Method	Extra	Backbone	Input size	AP	AP.5	AP.75	AP(M)	AP(L)
T	2017	[179]	no	ResNet-101	353×257	64.9	85.5	71.3	62.3	70.0
	2017	[179]	yes	ResNet-101	353×257	68.5	87.1	75.5	65.8	73.3
	2018	[30]	no	ResNet-Incep	384×288	72.1	91.4	80.0	68.7	77.2
	2018	[256]	no	ResNet-152	384×288	73.7	91.9	81.1	70.3	80.0
	2019	[218]	no	HRNet-W32	384×288	74.9	92.5	82.8	71.3	80.9
	2019	[218]	no	HRNet-W48	384×288	75.5	92.5	83.3	71.9	81.5
	2019	[218]	yes	HRNet-W48	384×288	77.0	92.7	84.5	73.4	83.1
	2019	[127]	yes	4xResNet-50	384×288	77.1	93.8	84.6	73.4	82.3
	2020	[276]	no	HRNet-W48	384×288	76.2	92.5	83.6	72.5	82.4
	2020	[276]	yes	HRNet-W48	384×288	77.4	92.6	84.6	73.6	83.7
	2020	[13]	no	4xResNet-50	384×288	78.6	94.3	86.6	75.5	83.3
	2021	[264]	no	HRNet-W48	256×192	75.0	92.2	82.3	71.3	81.1
	2021	[130]	no	HRNet-W48	384×288	75.9	92.3	83.4	72.2	82.1
	B	2017	[15]	no	-	-	61.8	84.9	67.5	57.1
2017		[169]	no	Hourglass	512×512	65.5	86.8	72.3	60.6	72.6
2018		[178]	no	ResNet-152	1401×1401	68.7	89.0	75.4	64.1	75.5
2019		[226]	no	ResNet-101	800×800	64.8	87.8	71.1	60.4	71.5
2019		[174]	no	Hourglass	384×384	66.9	88.5	72.9	62.6	73.1
2020		[90]	no	Hourglass	512×512	67.6	85.1	73.7	62.7	74.6
2020		[32]	no	HRNet-W48	640×640	70.5	89.3	77.2	66.6	75.8

Table 4. Datasets for 3D HPE.

Dataset	Year	Capture system	Environment	Size	Single person	Multi-person	Single view	Multi-view
HumanEva [215]	2010	Marker-based MoCap	Indoor	6 subject, 7 actions, 40k frames	Yes	No	Yes	Yes
Human3.6M [77]	2014	Marker-based MoCap	Indoor	11 subjects, 17 actions, 3.6M frames	Yes	No	Yes	Yes
CMU Panoptic [94]	2016	Marker-less MoCap	Indoor	8 subjects, 1.5M frames	Yes	Yes	Yes	Yes
MPI-INF-3DHP [156]	2017	Marker-less MoCap	Indoor and outdoor	8 subjects, 8 actions, 1.3M frames	Yes	No	Yes	Yes
TotalCapture [232]	2017	Marker-based MoCap with IMUs	Indoor	5 subjects, 5 actions, 1.9M frames	Yes	No	Yes	Yes
3DPW [240]	2018	Hand-held cameras with IMUs	Indoor and outdoor	7 subjects, 51k frames	Yes	Yes	Yes	No
Mu3TS-3D [158]	2018	Marker-less MoCap	Indoor and outdoor	8 subjects, 8k frames	Yes	Yes	Yes	Yes
AMASS [151]	2019	Marker-based MoCap	Indoor and outdoor	300 subjects, 9M frames	Yes	No	Yes	Yes
NBA2K [304]	2020	NBA2K19 game engine	Indoor	27 subjects, 27k poses	Yes	No	Yes	No
GTA-IM [14]	2020	GTA game engine	Indoor	1M frames	Yes	No	Yes	No
Occlusion-Person [287]	2020	Unreal Engine 4 game engine	Indoor	73k frames	Yes	No	Yes	Yes

the predicted keypoints is dependent on the resolution of heatmaps. The computational cost and memory footprint are significantly increased when using high resolution heatmaps[218].

Multi-person 2D HPE: Table 3 presents the experimental results of different 2D HPE methods on the test-dev set of the COCO dataset, together with a summary of the experiment settings (extra data, backbones in models, input image size) and AP scores for each approach. The comparison experiments highlight the significant results of both top-down and bottom-up methods in multi-person HPE. Presumably, the top-down pipeline yields better results because it first detects each individual from the image using detection methods, then predicts the locations of keypoints using single-person HPE approaches. In this case, the keypoint estimation for each detected person is made easier, as the background is largely removed. But on the other hand, bottom-up methods are generally faster than top-down methods, because they directly detect all the keypoints and group them into individual poses using keypoint association strategies such as affinity linking [15], associative embedding [169], and pixel-wise keypoint regression [300].

5.4 Datasets for 3D HPE

In contrast to numerous 2D human pose datasets with high-quality annotation, acquiring accurate 3D annotation for 3D HPE datasets is a challenging task that requires motion capture systems such as MoCap and wearable IMUs. Due to this requirement, many 3D pose datasets are created in constrained environments. Due to page limit, we only review several widely used large-scale 3D pose datasets for deep learning-based 3D HPE in the following.

Human3.6M [77] is the most widely used indoor dataset for 3D HPE from monocular images and videos. There are 11 professional actors (6 males and 5 females) performing 17 activities (e.g., smoking, taking photo, talking on the phone) from 4 different views in an indoor laboratory environment. This dataset contains 3.6 million 3D human poses with 3D ground truth annotation captured by accurate marker-based MoCap system. Protocol #1 uses images of subjects S1, S5, S6, and S7 for training, and images of subjects S9 and S11 for testing.

Table 5. Comparison of different 3D single-view single-person HPE approaches on the Human3.6M dataset (Protocol 1). In skeleton-only approaches, “Direct” indicates the methods directly estimating 3D pose without 2D pose representation. “Lifting” denotes the methods lifting the 2D pose representation to the 3D space.

Skeleton-only methods				MPJPE																PA-MPJPE		
Approaches	Year	Methods	2D pose detector	Input	Dir.	Disc.	Eat.	Greet	Phone	Photo	Pose	Purch.	Sit	SitD.	Somme	Wait	WalkD.	Walk	WalkF.	Average	Average	
Direct	2017	[183]	-	image	67.4	71.9	66.7	69.1	72.0	77.0	65.0	68.3	83.7	96.5	71.7	65.8	74.9	59.1	63.2	71.9	51.9	
	2018	[182]	-	image	48.5	54.4	54.4	52.0	59.4	65.3	49.9	52.9	65.8	71.1	56.6	52.9	60.9	44.7	47.8	47.8	56.2	41.8
	2017	[155]	Hourglass	image	53.8	56.2	58.1	59.0	69.5	78.4	55.2	58.1	74.0	94.6	62.3	59.1	65.1	49.5	52.4	62.9	47.7	42.6
	2019	[65]	own design	image	54.0	65.1	58.5	62.9	67.9	75.0	54.0	60.6	82.7	98.2	63.3	61.2	66.9	50.0	56.5	65.7	49.2	42.6
	2019	[117]	Hourglass	image	43.8	48.6	49.1	49.8	57.6	61.5	45.9	48.3	62.0	73.4	54.8	50.6	56.0	43.4	45.5	52.7	58.0	-
	2019	[214]	Hourglass	image	48.6	54.5	54.2	55.7	62.6	72.0	50.5	54.3	70.0	78.3	58.1	55.4	61.4	45.2	49.7	58.0	-	-
	2019	[288]	own design	image	47.3	60.7	51.4	60.5	61.1	49.9	47.3	68.1	86.2	35.0	67.8	61.0	42.1	60.6	45.3	57.6	-	-
	2021	[306]	CPN	image	45.4	49.2	45.7	49.4	50.4	58.2	47.9	46.0	57.5	63.0	49.7	46.6	52.2	38.9	40.8	49.4	39.1	36.3
	2018	[45]	Hourglass	Video	44.8	50.4	44.7	49.0	52.9	61.4	43.5	45.5	63.1	87.3	51.7	48.5	52.2	37.6	41.9	52.1	46.1	36.3
	2019	[186]	CPN	Video	45.2	46.7	43.3	45.6	48.1	55.1	44.6	44.3	57.3	65.8	47.1	44.0	49.0	32.8	33.9	42.8	36.5	35.0
Lifting	2019	[12]	CPN	Video	44.6	47.4	45.6	48.8	50.8	59.0	47.2	43.9	57.9	61.9	49.7	46.6	51.3	37.1	39.4	44.8	39.0	35.6
	2020	[141]	CPN	Video	41.8	44.8	41.1	44.9	47.4	54.1	43.4	42.2	56.2	63.6	45.3	45.3	31.3	32.2	45.1	35.6	-	-
	2020	[274]	CPN	Video	46.6	47.1	43.9	41.6	45.8	49.6	46.5	40.0	53.4	61.1	46.1	43.6	43.1	31.5	32.6	44.8	-	-
	2020	[247]	HRNet	Video	38.2	41.0	45.9	39.7	41.4	51.4	41.6	41.4	52.0	57.4	41.8	44.4	41.6	33.1	30.0	42.6	32.7	32.7
	2020	[22]	CPN	Video	41.4	43.5	40.1	42.9	46.6	51.9	41.7	42.3	53.9	60.2	45.4	41.7	46.0	31.5	32.7	44.1	35.0	35.0
	2021	[294]	CPN	Video	41.5	44.8	39.8	42.5	46.5	51.6	42.1	42.0	53.3	60.7	45.5	43.3	46.1	31.8	32.2	44.3	34.6	34.6
	2021	[126]	CPN	Video	39.2	43.1	40.1	40.9	44.9	51.2	40.6	41.3	53.5	60.3	43.7	41.1	43.8	29.8	30.6	43.0	43.0	43.0
	Human mesh recovery methods				MPJPE																PA-MPJPE	
	output	Year	Methods	Model	Input	Dir.	Disc.	Eat.	Greet	Phone	Photo	Pose	Purch.	Sit	SitD.	Somme	Wait	WalkD.	Walk	WalkF.	Average	Average
	Mesh	2018	[99]	SMPL	Image	-	-	-	-	-	-	-	-	-	-	-	-	-	-	-	-	88.0
2019		[107]	SMPL	Image	-	-	-	-	-	-	-	-	-	-	-	-	-	-	-	-	-	50.1
2019		[106]	SMPL	Image	-	-	-	-	-	-	-	-	-	-	-	-	-	-	-	-	-	41.1
2019		[255]	Adam	Image	-	-	-	-	-	-	-	-	-	-	-	-	-	-	-	-	-	58.3
2020		[38]	SMPL	Image	-	-	-	-	-	-	-	-	-	-	-	-	-	-	-	-	-	64.9
2021		[280]	SMPL	Image	-	-	-	-	-	-	-	-	-	-	-	-	-	-	-	-	-	57.7
2021		[135]	SMPL	Image	-	-	-	-	-	-	-	-	-	-	-	-	-	-	-	-	-	54.0
2021		[136]	SMPL	Image	-	-	-	-	-	-	-	-	-	-	-	-	-	-	-	-	-	51.2
2019		[5]	SMPL	Video	-	-	-	-	-	-	-	-	-	-	-	-	-	-	-	-	-	77.8
2020		[103]	SMPL	Video	-	-	-	-	-	-	-	-	-	-	-	-	-	-	-	-	-	65.6
2021	[37]	SMPL	Video	-	-	-	-	-	-	-	-	-	-	-	-	-	-	-	-	-	62.3	

MPI-INF-3DHP [156] is captured by a commercial marker-less MoCap system in a multi-camera studio. There are 8 actors (4 males and 4 females) performing 8 human activities including walking, sitting, complex exercise posed, and dynamic actions. More than 1.3 million frames from 14 cameras were recorded in a green screen studio which allows automatic segmentation and augmentation.

MuPoTS-3D [158] is a multi-person 3D test set and its ground-truth 3D poses were captured by a multi-view marker-less MoCap system containing 20 real-world scenes (5 indoor and 15 outdoor). There are challenging samples with occlusions, drastic illumination changes, and lens flares in some of the outdoor footage. More than 8,000 frames were collected in the 20 sequences by 8 subjects.

Readers are referred to the original references for details about other datasets including **HumanEva** [215], **CMU Panoptic Dataset** [94], **TotalCapture** [232], **MuCo-3DHP Dataset** [158], **3DPW** [240], **AMASS** [151], **NBA2K** [304], **GTA-IM** [14], and **Occlusion-Person** [287]. A summary of these datasets is shown in Table 4.

5.5 Evaluation Metrics for 3D HPE

MPJPE (Mean Per Joint Position Error) is the most widely used metric to evaluate the performance of 3D HPE. MPJPE is computed by using the Euclidean distance between the estimated 3D joints and the ground truth positions as follows:

$$MPJPE = \frac{1}{N} \sum_{i=1}^N \|J_i - J_i^*\|_2, \quad (1)$$

where N is the number of joints, J_i and J_i^* are the ground truth position and the estimated position of the i_{th} joint.

PMPJPE, also called Reconstruction Error, is the MPJPE after rigid alignment by a post-processing between the estimated pose and the ground truth pose.

NMPJPE is defined as the MPJPE after normalizing the predicted positions in scale to the reference [205].

MPVE (Mean Per Vertex Error) [185] measures the Euclidean distances between the ground truth vertices and the predicted vertices as follows:

$$MPVE = \frac{1}{N} \sum_{i=1}^N \|V_i - V_i^*\|_2, \quad (2)$$

where N is the number of vertices, V is the ground truth vertices, and V^* is the estimated vertices.

3DPCK is a 3D extended version of the Percentage of Correct Keypoints (PCK) metric used in 2D HPE evaluation. An estimated joint is considered as correct if the distance between the estimation and the ground-truth is within a certain threshold. Generally the threshold is set to 150mm.

Table 6. Comparison of different 3D single-view multi-person HPE approaches on the MuPoTS-3D dataset.

		MuPoTS-3D		
		Method	3DPCK \uparrow	
			All people	Matched people
Top down	2019	[207]	70.6	74.0
	2019	[164]	81.8	82.5
	2020	[89]	69.1	72.2
	2020	[118]	82.0	-
	2021	[33]	87.5	-
Bottom up	2018	[158]	65.0	69.8
	2019	[157]	70.4	-
	2020	[8]	72.0	-
	2020	[292]	73.5	80.5
	Integrated	2021	[34]	89.6

Table 7. Comparison of different 3D multi-view HPE approaches on the Human3.6M dataset.

		Human3.6M			
Year	Method	Use extra 3D data	Protocol 1		Protocol 1
			MPJPE \downarrow	Normalized MPJPE \downarrow	PA-MPJPE \downarrow
2019	[133]	Yes	79.9	-	45.1
2019	[105]	No	60.6	60.0	47.5
2019	[197]	No	31.2	-	-
2019	[197]	Yes	26.2	-	-
2020	[202]	No	30.2	-	-
2020	[257]	No	29.3	-	-
2020	[287]	Yes	19.5	-	-
2021	[149]	No	25.8	-	-
2021	[201]	Yes	18.7	-	-

Summary. As pointed out by Ji et al. [85], low MPJPE does not always indicate an accurate pose estimation as it depends on the predicted scale of human shape and skeleton. Although 3DPCK is more robust to incorrect joints, it cannot evaluate the precision of correct joints. Existing metrics are designed to evaluate the precision of an estimated pose in a single frame. However, the temporal consistency and smoothness of reconstructed human pose cannot be examined over continuous frames by existing evaluation metrics. Designing frame-level evaluation metrics that can evaluate 3D HPE performance with temporal consistency and smoothness remains an open problem.

5.6 Performance Comparison of 3D HPE Methods

Single-view single-person: In Table 5, it is seen that most 3D single-view single-person HPE methods estimate 3D human pose with remarkable precision on the Human3.6M dataset. However, despite the fact that the Human3.6M dataset has a large size of training and testing data, it only contains 11 actors performing 17 activities in lab environments. When estimating 3D pose on the in-the-wild data with more complex scenarios, the performance of these methods degrades quickly. Estimating 3D pose from videos can achieve better performance than from a single image because the temporal consistency is preserved.

For skeleton-only methods, 2D-to-3D lifting approaches generally outperform direct estimation approaches due to the excellent performance of state-of-the-art 2D pose detectors. Beyond estimated 3D coordinates of joints, a group of methods utilized volumetric models such as SMPL to recover human mesh. These methods still reported MPJPE of joints since the datasets do not provide the ground truth mesh vertices. However, the reported MPJPE are higher than those methods only estimating 3D joints. One of the reasons is that these methods regressed pose parameters and shape parameters jointly then fed in the volumetric model for mesh reconstruction, only evaluating MPJPE of joints can not show their strength.

Single-view multi-person: Estimating 3D pose of multi-person is a harder task than single-person due to more severe occlusion. As shown in Tables 6, good progress has been made in single-view multi-person HPE methods in recent years. The Top-Down methods perform better than Bottom-Up methods due to the state-of-the-art person detection methods and single-person HPE methods. On the other hand, Bottom-Up methods are more computation and time efficient.

Multi-view: By comparing the results from Table 5 and Table 7, it is evident that the performance (e.g., MPJPE under Protocol 1) of multi-view 3D HPE methods has improved compared to single-view 3D HPE methods using the same dataset and evaluation metric. Occlusion and depth ambiguity can be alleviated through multi-view setting.

6 APPLICATIONS

In this section, we review related works of exploring HPE for a few popular applications.

Action recognition, prediction, detection, and tracking: Pose information has been utilized as cues for various applications such as action recognition, prediction, detection, and tracking. Angelini et al. [4] proposed a real-time action recognition method using a pose-based algorithm. Yan et al. [263] leveraged the dynamic skeleton modality of pose for action recognition. Markovitz et al. [154] studied human pose graphs for anomaly detection of human actions in videos. Cao et al. [14] used the predicted 3D pose for long-term human motion prediction. Sun et al. [217] proposed a view-invariant probabilistic pose embedding for video alignment.

Pose-based video surveillance enjoys the advantage of preserving privacy by monitoring through pose and human mesh representation instead of human sensitive identities. Das et al. [46] embedded video with pose to identify activities of daily living for monitoring human behavior.

Action correction and online coaching: Some activities such as dancing, sporting, and professional training require precise human body control to strictly react as the standard pose. Normally personal trainers are responsible for the pose correction and action guidance in a face-to-face manner. With the help of 3D HPE and action detection, AI personal trainers can make coaching more convenient by simply setting up cameras without a personal trainer presenting. Wang et al. [246] designed an AI coaching system with a pose estimation module for personalized athletic training assistance.

Clothes parsing: The e-commerce trends have brought about a noticeable impact on various aspects including clothes purchases. Clothing product in pictures can no longer satisfy customers' demands, and customers hope to see the reliable appearance as they wear their selected clothes. Clothes parsing [270] [210] and pose transfer [129] make it possible by inferring the 3D appearance of a person wearing a specific clothes. HPE can provide plausible human body regions for cloth parsing. Moreover, the recommendation system can be upgraded by evaluating appropriateness based on the inferred reliable 3D appearance of customers with selected items. Patel et al. [180] achieved clothing prediction from 3D pose, shape and garment style.

Animation, movie, and gaming: Motion capture is the key component to present characters with complex movements and realistic physical interactions in industries of animation, movie, and gaming. The motion capture devices are usually expensive and complicated to set up. HPE can provide realistic pose information while alleviating the demand for professional high-cost equipment [253][139].

AR and VR: Augmented Reality (AR) technology aims to enhance the interactive experience of digital objects into the real-world environment. The objective of Virtual Reality (VR) technology is to provide an immersive experience for the users. AR and VR devices use human pose information as input to achieve their goals of different applications. A cartoon character can be generated in real-world scenes to replace the real person. Weng et al. [252] created 3D character animation from single photo with the help of 3D pose estimation and human mesh recovery. Zhang et al. [279] presented a pose-based system that converts broadcast tennis match videos into interactive and controllable video sprites.

Healthcare: HPE provides quantitative human motion information that physicians can diagnose some complex diseases, create rehabilitation training, and operate physical therapy. Lu et al. [145] designed a pose-based estimation system for assessing Parkinson's disease motor severity. Gu et al. [63] developed a pose-based physical therapy system that patients can be evaluated and advised at home. Furthermore, such a system can be established to detect abnormal action and to predict the following actions ahead of time. Alerts are sent immediately if the system determines that danger may occur. Chen et al. [24] used the HPE algorithms for fall detection monitoring in order

to provide immediate assistant. Also, HPE methods can provide reliable posture labels of patients in hospital environments to augment research on neural correlates to natural behaviors [20].

7 CONCLUSION AND FUTURE DIRECTIONS

In this survey, we have presented a systematic overview of recent deep learning-based 2D and 3D HPE methods. A comprehensive taxonomy and performance comparison of these methods have been covered. Despite great success, there are still many challenges as discussed in Sections 3.3 and 4.3. We further point out a few promising future directions to promote advances in HPE research.

- Domain adaptation for HPE. For some applications such as estimating human pose from infant images [73] or artwork collections [150], there are not enough training data with ground truth annotations. Moreover, data for these applications exhibit different distributions from that of the standard pose datasets. HPE methods trained on existing standard datasets may not generalize well across different domains. The recent trend to alleviate the domain gap is utilizing GAN-based learning approaches. Nonetheless, how to effectively transfer the human pose knowledge to bridge domain gaps remains unaddressed.
- Human body models such as SMPL, SMPL-X, GHUM & GHUML, and Adam are used to model human mesh representation. However, these models have a huge number of parameters. How to reduce the number of parameters while preserving the reconstructed mesh quality is an intriguing problem. Also, different people have various deformations of body shape. A more effective human body model may utilize other information such as BMI [176] and silhouette [131] for better generalization.
- Most existing methods ignore human interaction with 3D scenes. There are strong human-scene relationship constraints that can be explored such as a human subject cannot be simultaneously present in the locations of other objects in the scene. The physical constraints with semantic cues can provide reliable and realistic 3D HPE.
- 3D HPE is employed in visual tracking and analysis. Existing 3D human pose and shape reconstruction from videos are not smooth and continuous. One reason is that the evaluation metrics such as MPJPE cannot evaluate the smoothness and the degree of realisticness. Appropriate frame-level evaluation metrics focusing on temporal consistency and motion smoothness should be developed.
- Existing well-trained networks pay less attention to resolution mismatch. The training data of HPE networks are usually high resolution images or videos, which may lead to inaccurate estimation when predicting human pose from low resolution input. The contrastive learning scheme [23] (e.g., the original image and its low resolution version as a positive pair) might be helpful for building resolution-aware HPE networks.
- Deep neural networks in vision tasks are vulnerable to adversarial attacks. The imperceptible noise can significantly affect the performance of HPE. There are few works [138] [83] that consider adversarial attack for HPE. The study of defense against adversarial attacks can improve the robustness of HPE networks and facilitate real-world pose-based applications.
- Human body parts may have different movement patterns and shapes due to the heterogeneity of the human body. A single shared network architecture may not be optimal for estimating all body parts with various degrees of freedom. Neural Architecture Search (NAS) [52] can search the optimal architecture for estimating each body part [31]. Also, NAS can be used for discovering efficient HPE network architectures to reduce the computational cost [282]. It is also worth exploring multi-objective NAS in HPE when multiple objectives (e.g, latency, accuracy and energy consumption) have to be met.

HPE workshops and challenges: Finally, we list the HPE workshops and challenges (2017-2021) in Table 8 to facilitate research in this field.

Table 8. Workshops and challenges for 2D and 3D HPE.

ICCV 2017	PoseTrack Challenge: Human Pose Estimation and Tracking in the Wild Link
ECCV 2018	PoseTrack Challenge: Articulated People Tracking in the Wild Link
CVPR 2018	3D humans 2018: 1st International workshop on Human pose, motion, activities and shape Link
CVPR 2019	3D humans 2019: 2nd International workshop on Human pose, motion, activities and shape Link
CVPR 2019	Workshop On Augmented Human: Human-centric Understanding Link
CVPR 2020	Towards Human-Centric Image/Video Synthesis Link
ECCV 2020	3D poses in the wild challenge Link
ACM MM 2020	Large-scale Human-centric Video Analysis in Complex Events Link
ICCV 2021	Benchmark and Challenge on Human Trajectory and Pose Dynamics Forecasting in the Wild Link

REFERENCES

- [1] [n. d.]. *MSCOCO keypoint detection evaluation metric*. <https://cocodataset.org/#keypoints-eval> (2016).
- [2] M. Andriluka, U. Iqbal, E. Ensafutdinov, L. Pishchulin, A. Milan, J. Gall, and Schiele B. 2018. PoseTrack: A Benchmark for Human Pose Estimation and Tracking. In *CVPR*.
- [3] Mykhaylo Andriluka, Leonid Pishchulin, Peter Gehler, and Bernt Schiele. 2014. 2d human pose estimation: New benchmark and state of the art analysis. In *CVPR*.
- [4] Federico Angelini, Zeyu Fu, Yang Long, Ling Shao, and Syed Mohsen Naqvi. 2018. Actionxpose: A novel 2d multi-view pose-based algorithm for real-time human action recognition. *arXiv preprint arXiv:1810.12126* (2018).
- [5] Anurag Arnab, Carl Doersch, and Andrew Zisserman. 2019. Exploiting Temporal Context for 3D Human Pose Estimation in the Wild. In *CVPR*.
- [6] Bruno Artacho and Andreas Savakis. 2020. UniPose: Unified Human Pose Estimation in Single Images and Videos. In *CVPR*.
- [7] Vasileios Belagiannis and Andrew Zisserman. 2017. Recurrent human pose estimation. In *FG*.
- [8] Abdallah Benzine, Florian Chabot, Bertrand Luvison, Quoc Cuong Pham, and Catherine Achard. 2020. PandaNet: Anchor-Based Single-Shot Multi-Person 3D Pose Estimation. In *CVPR*.
- [9] Federica Bogo, Angjoo Kanazawa, Christoph Lassner, Peter Gehler, Javier Romero, and Michael J. Black. 2016. Keep it SMPL: Automatic Estimation of 3D Human Pose and Shape from a Single Image. In *ECCV*.
- [10] Adrian Bulat and Georgios Tzimiropoulos. 2016. Human pose estimation via convolutional part heatmap regression. In *ECCV*.
- [11] M. Burenius, J. Sullivan, and S. Carlsson. 2013. 3D Pictorial Structures for Multiple View Articulated Pose Estimation. In *CVPR*.
- [12] Y. Cai, L. Ge, J. Liu, J. Cai, T. Cham, J. Yuan, and N. M. Thalmann. 2019. Exploiting Spatial-Temporal Relationships for 3D Pose Estimation via Graph Convolutional Networks. In *ICCV*.
- [13] Yuanhao Cai, Zhicheng Wang, Zhengxiong Luo, Binyi Yin, Angang Du, Haoqian Wang, Xinyu Zhou, Erjin Zhou, Xiangyu Zhang, and Jian Sun. 2020. Learning Delicate Local Representations for Multi-Person Pose Estimation. *arXiv preprint arXiv:2003.04030* (2020).
- [14] Zhe Cao, Hang Gao, Karttikeya Mangalam, Qizhi Cai, Minh Vo, and Jitendra Malik. 2020. Long-term human motion prediction with scene context. In *ECCV*.
- [15] Zhe Cao, Tomas Simon, Shih-En Wei, and Yaser Sheikh. 2017. Realtime multi-person 2d pose estimation using part affinity fields. In *CVPR*.
- [16] Joao Carreira, Pulkit Agrawal, Katerina Fragkiadaki, and Jitendra Malik. 2016. Human pose estimation with iterative error feedback. In *CVPR*.
- [17] Ching-Hang Chen and Deva Ramanan. 2017. 3D Human Pose Estimation = 2D Pose Estimation + Matching. *CVPR* (2017).
- [18] Ching-Hang Chen, Amrbrish Tyagi, Amit Agrawal, Dylan Drover, Rohith MV, Stefan Stojanov, and James M. Rehg. 2019. Unsupervised 3D Pose Estimation With Geometric Self-Supervision. In *CVPR*.
- [19] He Chen, Pengfei Guo, Pengfei Li, Gim Hee Lee, and Gregory Chirikjian. 2020. Multi-person 3D Pose Estimation in Crowded Scenes Based on Multi-View Geometry. In *ECCV*.
- [20] Kenny Chen, Paolo Gabriel, Abdulwahab Alasfour, Chenghao Gong, Werner K Doyle, Orrin Devinsky, Daniel Friedman, Patricia Dugan, Lucia Melloni, Thomas Thesen, et al. 2018. Patient-specific pose estimation in clinical environments. *JTEHM* (2018).
- [21] Long Chen, Haizhou Ai, Rui Chen, Zijie Zhuang, and Shuang Liu. 2020. Cross-View Tracking for Multi-Human 3D Pose Estimation at Over 100 FPS. In *CVPR*.
- [22] Tianlang Chen, Chen Fang, Xiaohui Shen, Yiheng Zhu, Zhili Chen, and Jiebo Luo. 2021. Anatomy-aware 3D Human Pose Estimation with Bone-based Pose Decomposition. *TCSVT* (2021).

- [23] Ting Chen, Simon Kornblith, Mohammad Norouzi, and Geoffrey Hinton. 2020. A simple framework for contrastive learning of visual representations. *arXiv preprint arXiv:2002.05709* (2020).
- [24] Weiming Chen, Zijie Jiang, Hailin Guo, and Xiaoyang Ni. 2020. Fall Detection Based on Key Points of Human-Skeleton Using OpenPose. *Symmetry* (2020).
- [25] X. Chen, K. Lin, W. Liu, C. Qian, and L. Lin. 2019. Weakly-Supervised Discovery of Geometry-Aware Representation for 3D Human Pose Estimation. In *CVPR*.
- [26] Xianjie Chen and Alan L Yuille. 2014. Articulated pose estimation by a graphical model with image dependent pairwise relations. In *NeurIPS*.
- [27] Xianjie Chen and Alan L Yuille. 2015. Parsing occluded people by flexible compositions. In *CVPR*.
- [28] Yu Chen, Chunhua Shen, Xiu-Shen Wei, Lingqiao Liu, and Jian Yang. 2017. Adversarial posenet: A structure-aware convolutional network for human pose estimation. In *ICCV*.
- [29] Yucheng Chen, Yingli Tian, and Mingyi He. 2020. Monocular human pose estimation: A survey of deep learning-based methods. *CVIU* (2020).
- [30] Yilun Chen, Zhicheng Wang, Yuxiang Peng, Zhiqiang Zhang, Gang Yu, and Jian Sun. 2018. Cascaded pyramid network for multi-person pose estimation. In *CVPR*.
- [31] Zerui Chen, Yan Huang, Hongyuan Yu, Bin Xue, Ke Han, Yiru Guo, and Liang Wang. 2020. Towards Part-aware Monocular 3D Human Pose Estimation: An Architecture Search Approach. In *ECCV*.
- [32] Bowen Cheng, Bin Xiao, Jingdong Wang, Honghui Shi, Thomas S Huang, and Lei Zhang. 2019. HigherHRNet: Scale-Aware Representation Learning for Bottom-Up Human Pose Estimation. *arXiv preprint arXiv:1908.10357* (2019).
- [33] Yu Cheng, Bo Wang, Bo Yang, and Robby T. Tan. 2021. Graph and Temporal Convolutional Networks for 3D Multi-person Pose Estimation in Monocular Videos. *AAAI* 35, 2 (May 2021), 1157–1165.
- [34] Yu Cheng, Bo Wang, Bo Yang, and Robby T. Tan. 2021. Monocular 3D Multi-Person Pose Estimation by Integrating Top-Down and Bottom-Up Networks. In *CVPR*. 7649–7659.
- [35] Y. Cheng, B. Yang, B. Wang, Y. Wending, and R. Tan. 2019. Occlusion-Aware Networks for 3D Human Pose Estimation in Video. In *ICCV*.
- [36] Yu Cheng, Bo Yang, Bo Wang, Wending Yan, and Robby T. Tan. 2019. Occlusion-Aware Networks for 3D Human Pose Estimation in Video. In *ICCV*.
- [37] Hongsuk Choi, Gyeongsik Moon, Ju Yong Chang, and Kyoung Mu Lee. 2021. Beyond Static Features for Temporally Consistent 3D Human Pose and Shape From a Video. In *CVPR*. 1964–1973.
- [38] Hongsuk Choi, Gyeongsik Moon, and Kyoung Mu Lee. 2020. Pose2Mesh: Graph Convolutional Network for 3D Human Pose and Mesh Recovery from a 2D Human Pose. In *ECCV*.
- [39] Chia-Jung Chou, Jui-Ting Chien, and Hwann-Tzong Chen. 2018. Self adversarial training for human pose estimation. In *APSIPA ASC*.
- [40] Xiao Chu, Wanli Ouyang, Hongsheng Li, and Xiaogang Wang. 2016. Structured feature learning for pose estimation. In *CVPR*.
- [41] Xiao Chu, Wei Yang, Wanli Ouyang, Cheng Ma, Alan L Yuille, and Xiaogang Wang. 2017. Multi-context attention for human pose estimation. In *CVPR*.
- [42] H. Ci, C. Wang, X. Ma, and Y. Wang. 2019. Optimizing Network Structure for 3D Human Pose Estimation. In *ICCV*.
- [43] Henry M. Clever, Zackory Erickson, Ariel Kapusta, Greg Turk, Karen Liu, and Charles C. Kemp. 2020. Bodies at Rest: 3D Human Pose and Shape Estimation From a Pressure Image Using Synthetic Data. In *CVPR*.
- [44] Timothy F Cootes, Christopher J Taylor, David H Cooper, and Jim Graham. 1995. Active shape models-their training and application. *CVIU* (1995).
- [45] Rishabh Dabral, Anurag Mundhada, Uday Kusupati, Safeer Afaque, Abhishek Sharma, and Arjun Jain. 2018. Learning 3D Human Pose from Structure and Motion. In *ECCV*.
- [46] Srijan Das, Saurav Sharma, Rui Dai, François Brémond, and Monique Thonnat. 2020. VPN: Learning Video-Pose Embedding for Activities of Daily Living. In *ECCV*.
- [47] Bappaditya Debnath, Mary O'Brien, Motonori Yamaguchi, and Ardhendu Behera. 2018. Adapting MobileNets for mobile based upper body pose estimation. In *AVSS*.
- [48] Junting Dong, Wen Jiang, Qixing Huang, Hujun Bao, and Xiaowei Zhou. 2019. Fast and Robust Multi-Person 3D Pose Estimation From Multiple Views. In *CVPR*.
- [49] Zijian Dong, Jie Song, Xu Chen, Chen Guo, and Otmar Hilliges. 2021. Shape-aware Multi-Person Pose Estimation from Multi-view Images. In *International Conference on Computer Vision (ICCV)*.
- [50] Dylan Drover, Ching-Hang Chen, Amit Agrawal, Amrith Tyagi, and Cong Phuoc Huynh. 2018. Can 3d pose be learned from 2d projections alone?. In *ECCV*.
- [51] Marcin Eichner, Manuel Marin-Jimenez, Andrew Zisserman, and Vittorio Ferrari. 2012. 2d articulated human pose estimation and retrieval in (almost) unconstrained still images. *IJCV* (2012).
- [52] Thomas Elsken, Jan Hendrik Metzen, and Frank Hutter. 2019. Neural Architecture Search: A Survey. *JMLR* (2019).

- [53] Matteo Fabbri, Fabio Lanzi, Simone Calderara, Stefano Alletto, and Rita Cucchiara. 2020. Compressed Volumetric Heatmaps for Multi-Person 3D Pose Estimation. In *CVPR*.
- [54] Xiaochuan Fan, Kang Zheng, Yuewei Lin, and Song Wang. 2015. Combining local appearance and holistic view: Dual-source deep neural networks for human pose estimation. In *CVPR*.
- [55] Hao-Shu Fang, Shuqin Xie, Yu-Wing Tai, and Cewu Lu. 2017. Rmpe: Regional multi-person pose estimation. In *ICCV*.
- [56] Mihai Fieraru, Anna Khoreva, Leonid Pishchulin, and Bernt Schiele. 2018. Learning to refine human pose estimation. In *CVPR Workshops*.
- [57] Martin Fisch and Ronald Clark. 2020. Orientation Keypoints for 6D Human Pose Estimation. *arXiv preprint arXiv:2009.04930* (2020).
- [58] Oren Freifeld, Alexander Weiss, Silvia Zuffi, and Michael J Black. 2010. Contour people: A parameterized model of 2D articulated human shape. In *CVPR*.
- [59] Georgios Georgakis, Ren Li, Srikrishna Karanam, Terrence Chen, Jana Kosecka, and Ziyang Wu. 2020. Hierarchical Kinematic Human Mesh Recovery. In *ECCV*.
- [60] Georgia Gkioxari, Alexander Toshev, and Navdeep Jaitly. 2016. Chained predictions using convolutional neural networks. In *ECCV*.
- [61] Wenjuan Gong, Xuena Zhang, Jordi González, Andrews Sobral, Thierry Bouwmans, Changhe Tu, and El-hadi Zahzah. 2016. Human pose estimation from monocular images: A comprehensive survey. *Sensors* (2016).
- [62] Ian Goodfellow, Jean Pouget-Abadie, Mehdi Mirza, Bing Xu, David Warde-Farley, Sherjil Ozair, Aaron Courville, and Yoshua Bengio. 2014. Generative adversarial nets. In *NeurIPS*.
- [63] Yiwen Gu, Shreya Pandit, Elham Saraee, Timothy Nordahl, Terry Ellis, and Margrit Betke. 2019. Home-based physical therapy with an interactive computer vision system. In *ICCV Workshops*.
- [64] Marc Habermann, Weipeng Xu, Michael Zollhoefer, Gerard Pons-Moll, and Christian Theobalt. 2020. DeepCap: Monocular Human Performance Capture Using Weak Supervision. In *CVPR*.
- [65] I. Habibi, W. Xu, D. Mehta, G. Pons-Moll, and C. Theobalt. 2019. In the Wild Human Pose Estimation Using Explicit 2D Features and Intermediate 3D Representations. In *CVPR*.
- [66] Mohamed Hassan, Vasileios Choutas, Dimitrios Tzionas, and Michael J. Black. 2019. Resolving 3D Human Pose Ambiguities with 3D Scene Constraints. In *ICCV*.
- [67] Kaiming He, Xiangyu Zhang, Shaoqing Ren, and Jian Sun. 2016. Deep residual learning for image recognition. In *CVPR*.
- [68] Michael B Holte, Cuong Tran, Mohan M Trivedi, and Thomas B Moeslund. 2012. Human pose estimation and activity recognition from multi-view videos: Comparative explorations of recent developments. *IEEE J Sel Top Signal Process* (2012).
- [69] Congzhenhao Huang, Shuai Jiang, Yang Li, Ziyue Zhang, Jason Traish, Chen Deng, Sam Ferguson, and Richard Yi Da Xu. 2020. End-to-end Dynamic Matching Network for Multi-view Multi-person 3d Pose Estimation. In *ECCV*.
- [70] Fuyang Huang, Ailing Zeng, Minhao Liu, Qiuxia Lai, and Qiang Xu. 2020. DeepFuse: An IMU-Aware Network for Real-Time 3D Human Pose Estimation from Multi-View Image. In *WACV*.
- [71] Junjie Huang, Zheng Zhu, Feng Guo, and Guan Huang. 2020. The Devil is in the Details: Delving into Unbiased Data Processing for Human Pose Estimation. In *CVPR*.
- [72] Shaoli Huang, Mingming Gong, and Dacheng Tao. 2017. A coarse-fine network for keypoint localization. In *ICCV*.
- [73] Xiaofei Huang, Nihang Fu, Shuangjun Liu, Kathan Vyas, Amirreza Farnoosh, and Sarah Ostadabbas. 2020. Invariant Representation Learning for Infant Pose Estimation with Small Data. *arXiv preprint arXiv:2010.06100* (2020).
- [74] Yinghao Huang, Manuel Kaufmann, Emre Aksan, Michael J. Black, Otmar Hilliges, and Gerard Pons-Moll. 2018. Deep Inertial Poser: Learning to Reconstruct Human Pose from Sparse Inertial Measurements in Real Time. *ACM TOG* (2018).
- [75] Eldar Insafutdinov, Mykhaylo Andriluka, Leonid Pishchulin, Siyu Tang, Evgeny Levinkov, Bjoern Andres, and Bernt Schiele. 2017. Arttrack: Articulated multi-person tracking in the wild. In *CVPR*.
- [76] Eldar Insafutdinov, Leonid Pishchulin, Bjoern Andres, Mykhaylo Andriluka, and Bernt Schiele. 2016. Deepcruc: A deeper, stronger, and faster multi-person pose estimation model. In *ECCV*.
- [77] C. Ionescu, D. Papava, V. Olaru, and C. Sminchisescu. 2014. Human3.6M: Large Scale Datasets and Predictive Methods for 3D Human Sensing in Natural Environments. *IEEE TPAMI* (2014).
- [78] Umar Iqbal and Juergen Gall. 2016. Multi-person pose estimation with local joint-to-person associations. In *ECCV*.
- [79] Umar Iqbal, Pavlo Molchanov, and Jan Kautz. 2020. Weakly-Supervised 3D Human Pose Learning via Multi-View Images in the Wild. In *CVPR*.
- [80] Mariko Isogawa, Ye Yuan, Matthew O'Toole, and Kris M. Kitani. 2020. Optical Non-Line-of-Sight Physics-Based 3D Human Pose Estimation. In *CVPR*.
- [81] Ehsan Jahangiri and Alan L Yuille. 2017. Generating multiple diverse hypotheses for human 3d pose consistent with 2d joint detections. In *ICCV Workshops*.

- [82] Arjun Jain, Jonathan Tompson, Yann LeCun, and Christoph Bregler. 2014. Modeep: A deep learning framework using motion features for human pose estimation. In *ACCV*.
- [83] Naman Jain, Sahil Shah, Abhishek Kumar, and Arjun Jain. 2019. On the Robustness of Human Pose Estimation. In *CVPR Workshops*.
- [84] H. Jhuang, J. Gall, S. Zuffi, C. Schmid, and M. J. Black. 2013. Towards understanding action recognition. In *ICCV*.
- [85] Xiaopeng Ji, Qi FANG, Junting DONG, Qing SHUAI, Wen JIANG, and Xiaowei ZHOU. 2020. A survey on monocular 3D human pose estimation. *Virtual Reality & Intelligent Hardware* (2020).
- [86] Xiaofei Ji and Honghai Liu. 2009. Advances in view-invariant human motion analysis: a review. *IEEE TSMC* (2009).
- [87] Hao Jiang. 2010. Finding human poses in videos using concurrent matching and segmentation. In *ACCV*.
- [88] Haiyong Jiang, Jianfei Cai, and Jianmin Zheng. 2019. Skeleton-Aware 3D Human Shape Reconstruction From Point Clouds. In *ICCV*.
- [89] Wen Jiang, Nikos Kolotouros, Georgios Pavlakos, Xiaowei Zhou, and Kostas Daniilidis. 2020. Coherent Reconstruction of Multiple Humans From a Single Image. In *CVPR*.
- [90] Sheng Jin, Wentao Liu, Enze Xie, Wenhai Wang, Chen Qian, Wanli Ouyang, and Ping Luo. 2020. Differentiable Hierarchical Graph Grouping for Multi-Person Pose Estimation. *arXiv preprint arXiv:2007.11864* (2020).
- [91] Sheng Jin, Lumin Xu, Jin Xu, Can Wang, Wentao Liu, Chen Qian, Wanli Ouyang, and Ping Luo. 2020. Whole-Body Human Pose Estimation in the Wild. *arXiv preprint arXiv:2007.11858* (2020).
- [92] Sam Johnson and Mark Everingham. 2010. Clustered Pose and Nonlinear Appearance Models for Human Pose Estimation.. In *BMVC*.
- [93] Sam Johnson and Mark Everingham. 2011. Learning effective human pose estimation from inaccurate annotation. In *CVPR*.
- [94] Hanbyul Joo, Tomas Simon, Xulong Li, Hao Liu, Lei Tan, Lin Gui, Sean Banerjee, Timothy Scott Godisart, Bart Nabbe, Iain Matthews, Takeo Kanade, Shohei Nobuhara, and Yaser Sheikh. 2017. Panoptic Studio: A Massively Multiview System for Social Interaction Capture. *IEEE TPAMI* (2017).
- [95] H. Joo, T. Simon, and Y. Sheikh. 2018. Total Capture: A 3D Deformation Model for Tracking Faces, Hands, and Bodies. In *CVPR*.
- [96] Shanon X Ju, Michael J Black, and Yaser Yacoob. 1996. Cardboard people: A parameterized model of articulated image motion. In *FG*.
- [97] A. Kadkhodamohammadi, A. Gangi, M. de Mathelin, and N. Padoy. 2017. A Multi-view RGB-D Approach for Human Pose Estimation in Operating Rooms. In *WACV*.
- [98] Abdolrahim Kadkhodamohammadi and Nicolas Padoy. 2018. A generalizable approach for multi-view 3d human pose regression. *arXiv preprint arXiv:1804.10462* (2018).
- [99] Angjoo Kanazawa, Michael J. Black, David W. Jacobs, and Jitendra Malik. 2018. End-to-end Recovery of Human Shape and Pose. In *Computer Vision and Pattern Recognition (CVPR)*.
- [100] Ladislav Kavan. 2014. Part I: direct skinning methods and deformation primitives. In *ACM SIGGRAPH*.
- [101] Lipeng Ke, Ming-Ching Chang, Honggang Qi, and Siwei Lyu. 2018. Multi-scale structure-aware network for human pose estimation. In *ECCV*.
- [102] Salman Khan, Muzammal Naseer, Munawar Hayat, Syed Waqas Zamir, Fahad Shahbaz Khan, and Mubarak Shah. 2021. Transformers in vision: A survey. *arXiv preprint arXiv:2101.01169* (2021).
- [103] Muhammed Kocabas, Nikos Athanasiou, and Michael J Black. 2020. VIBE: Video inference for human body pose and shape estimation. In *CVPR*.
- [104] Muhammed Kocabas, Salih Karagoz, and Emre Akbas. 2018. Multiposenet: Fast multi-person pose estimation using pose residual network. In *ECCV*.
- [105] Muhammed Kocabas, Salih Karagoz, and Emre Akbas. 2019. Self-Supervised Learning of 3D Human Pose Using Multi-View Geometry. In *CVPR*.
- [106] N. Kolotouros, G. Pavlakos, M. Black, and K. Daniilidis. 2019. Learning to Reconstruct 3D Human Pose and Shape via Model-Fitting in the Loop. In *ICCV*.
- [107] Nikos Kolotouros, Georgios Pavlakos, and Kostas Daniilidis. 2019. Convolutional Mesh Regression for Single-Image Human Shape Reconstruction. In *CVPR*.
- [108] Nikos Kolotouros, Georgios Pavlakos, Dinesh Jayaraman, and Kostas Daniilidis. 2021. Probabilistic Modeling for Human Mesh Recovery. In *ICCV*.
- [109] Sven Kreiss, Lorenzo Bertoni, and Alexandre Alahi. 2019. Pifpaf: Composite fields for human pose estimation. In *CVPR*.
- [110] Alex Krizhevsky, Ilya Sutskever, and Geoffrey E Hinton. 2012. Imagenet classification with deep convolutional neural networks. In *NeurIPS*.
- [111] Jogendra Nath Kundu, Mugalodi Rakesh, Varun Jampani, Rahul M Venkatesh, and R. Venkatesh Babu. 2020. Appearance Consensus Driven Self-Supervised Human Mesh Recovery. In *ECCV*.

- [112] Jogendra Nath Kundu, Ambareesh Revanur, Govind Vitthal Waghmare, Rahul Mysore Venkatesh, and R. Venkatesh Babu. 2020. Unsupervised Cross-Modal Alignment for Multi-Person 3D Pose Estimation. In *ECCV*.
- [113] Jogendra Nath Kundu, Siddharth Seth, Varun Jampani, Mugalodi Rakesh, R. Venkatesh Babu, and Anirban Chakraborty. 2020. Self-Supervised 3D Human Pose Estimation via Part Guided Novel Image Synthesis. In *CVPR*.
- [114] Jogendra Nath Kundu, Siddharth Seth, MV Rahul, Mugalodi Rakesh, Venkatesh Babu Radhakrishnan, and Anirban Chakraborty. 2020. Kinematic-Structure-Preserved Representation for Unsupervised 3D Human Pose Estimation.. In *AAAI*.
- [115] Christoph Lassner, Javier Romero, Martin Kiefel, Federica Bogo, Michael J. Black, and Peter V. Gehler. 2017. Unite the People: Closing the Loop Between 3D and 2D Human Representations. In *CVPR*.
- [116] Kyoungoh Lee, Inwoong Lee, and Sanghoon Lee. 2018. Propagating LSTM: 3D Pose Estimation based on Joint Interdependency. In *ECCV*.
- [117] Chen Li and Gim Hee Lee. 2019. Generating Multiple Hypotheses for 3D Human Pose Estimation With Mixture Density Network. In *CVPR*.
- [118] Jiefeng Li, Can Wang, Wentao Liu, Chen Qian, and Cewu Lu. 2020. HMOR: Hierarchical Multi-Person Ordinal Relations for Monocular Multi-Person 3D Pose Estimation. In *ECCV*.
- [119] Jiefeng Li, Can Wang, Hao Zhu, Yihuan Mao, Hao-Shu Fang, and Cewu Lu. 2019. Crowdpose: Efficient crowded scenes pose estimation and a new benchmark. In *ICCV*.
- [120] Jiefeng Li, Chao Xu, Zhicun Chen, Siyuan Bian, Lixin Yang, and Cewu Lu. 2021. HybrIK: A Hybrid Analytical-Neural Inverse Kinematics Solution for 3D Human Pose and Shape Estimation. In *CVPR*. 3383–3393.
- [121] Ke Li, Shijie Wang, Xiang Zhang, Yifan Xu, Weijian Xu, and Zhuowen Tu. 2021. Pose Recognition with Cascade Transformers. In *CVPR*. 1944–1953.
- [122] Sijin Li and Antoni B. Chan. 2014. 3D Human Pose Estimation from Monocular Images with Deep Convolutional Neural Network. In *ACCV*.
- [123] Sijin Li, Zhi-Qiang Liu, and Antoni B Chan. 2014. Heterogeneous multi-task learning for human pose estimation with deep convolutional neural network. In *CVPR Workshops*.
- [124] Sijin Li, Weichen Zhang, and Antoni B. Chan. 2015. Maximum-Margin Structured Learning With Deep Networks for 3D Human Pose Estimation. In *ICCV*.
- [125] Wenhao Li, Hong Liu, Runwei Ding, Mengyuan Liu, Pichao Wang, and Wenming Yang. 2022. Exploiting Temporal Contexts with Strided Transformer for 3D Human Pose Estimation. *IEEE Transactions on Multimedia* (2022).
- [126] Wenhao Li, Hong Liu, Hao Tang, Pichao Wang, and Luc Van Gool. 2021. MHFormer: Multi-Hypothesis Transformer for 3D Human Pose Estimation. *arXiv preprint arXiv:2111.12707* (2021).
- [127] Wenbo Li, Zhicheng Wang, Binyi Yin, Qixiang Peng, Yuming Du, Tianzi Xiao, Gang Yu, Hongtao Lu, Yichen Wei, and Jian Sun. 2019. Rethinking on multi-stage networks for human pose estimation. *arXiv preprint arXiv:1901.00148* (2019).
- [128] Yizhuo Li, Miao Hao, Zonglin Di, Nitesh Bharadwaj Gundavarapu, and Xiaolong Wang. 2021. Test-time personalization with a transformer for human pose estimation. *Advances in Neural Information Processing Systems* 34 (2021).
- [129] Yining Li, Chen Huang, and Chen Change Loy. 2019. Dense Intrinsic Appearance Flow for Human Pose Transfer. In *CVPR*.
- [130] Yanjie Li, Shoukui Zhang, Zhicheng Wang, Sen Yang, Wankou Yang, Shu-Tao Xia, and Erjin Zhou. 2021. TokenPose: Learning Keypoint Tokens for Human Pose Estimation. In *ICCV*. 11313–11322.
- [131] Zhongguo Li, Anders Heyden, and Magnus Oskarsson. 2020. A novel joint points and silhouette-based method to estimate 3D human pose and shape. *arXiv preprint arXiv:2012.06109* (2020).
- [132] Z. Li, X. Wang, F. Wang, and P. Jiang. 2019. On Boosting Single-Frame 3D Human Pose Estimation via Monocular Videos. In *ICCV*.
- [133] Junbang Liang and Ming C. Lin. 2019. Shape-Aware Human Pose and Shape Reconstruction Using Multi-View Images. In *ICCV*.
- [134] Ita Lifshitz, Ethan Fetaya, and Shimon Ullman. 2016. Human pose estimation using deep consensus voting. In *ECCV*.
- [135] Kevin Lin, Lijuan Wang, and Zicheng Liu. 2021. End-to-end human pose and mesh reconstruction with transformers. In *CVPR*. 1954–1963.
- [136] Kevin Lin, Lijuan Wang, and Zicheng Liu. 2021. Mesh Graphormer. In *ICCV*.
- [137] Tsung-Yi Lin, Michael Maire, Serge Belongie, James Hays, Pietro Perona, Deva Ramanan, Piotr Dollár, and C Lawrence Zitnick. 2014. Microsoft coco: Common objects in context. In *ECCV*.
- [138] Jian Liu, Naveed Akhtar, and Ajmal Mian. 2019. Adversarial Attack on Skeleton-based Human Action Recognition. *arXiv preprint arXiv:1909.06500* (2019).
- [139] Jingyuan Liu, Hongbo Fu, and Chiew-Lan Tai. 2020. PoseTween: Pose-driven Tween Animation. In *ACM UIST*.
- [140] Kenkun Liu, Rongqi Ding, Zhiming Zou, Le Wang, and Wei Tang. 2020. A Comprehensive Study of Weight Sharing in Graph Networks for 3D Human Pose Estimation. In *ECCV*.

- [141] Ruixu Liu, Ju Shen, He Wang, Chen Chen, Sen-ching Cheung, and Vijayan Asari. 2020. Attention Mechanism Exploits Temporal Contexts: Real-Time 3D Human Pose Reconstruction. In *CVPR*.
- [142] Zhao Liu, Jianke Zhu, Jiajun Bu, and Chun Chen. 2015. A survey of human pose estimation: the body parts parsing based methods. *JVCIR* (2015).
- [143] Jonathan Long, Evan Shelhamer, and Trevor Darrell. 2015. Fully Convolutional Networks for Semantic Segmentation. In *CVPR*.
- [144] Matthew Loper, Naureen Mahmood, Javier Romero, Gerard Pons-Moll, and Michael J. Black. 2015. SMPL: A Skinned Multi-Person Linear Model. *ACM TOG* (2015).
- [145] Mandy Lu, Kathleen Poston, Adolf Pfefferbaum, Edith V Sullivan, Li Fei-Fei, Kilian M Pohl, Juan Carlos Niebles, and Ehsan Adeli. 2020. Vision-based Estimation of MDS-UPDRS Gait Scores for Assessing Parkinson’s Disease Motor Severity. *arXiv preprint arXiv:2007.08920* (2020).
- [146] Yue Luo, Jimmy Ren, Zhouxia Wang, Wenxiu Sun, Jinshan Pan, Jianbo Liu, Jiahao Pang, and Liang Lin. 2018. Lstm pose machines. In *CVPR*.
- [147] Diogo C Luvizon, David Picard, and Hedi Tabia. 2018. 2d/3d pose estimation and action recognition using multitask deep learning. In *CVPR*.
- [148] Diogo C Luvizon, Hedi Tabia, and David Picard. 2019. Human pose regression by combining indirect part detection and contextual information. *Computers & Graphics* (2019).
- [149] Haoyu Ma, Liangjian Chen, Deying Kong, Zhe Wang, Xingwei Liu, Hao Tang, Xiangyi Yan, Yusheng Xie, Shih-Yao Lin, and Xiaohui Xie. 2021. Transfusion: Cross-view fusion with transformer for 3d human pose estimation. *BMVC* (2021).
- [150] Prathmesh Madhu, Angel Villar-Corrales, Ronak Kosti, Torsten Bendschus, Corinna Reinhardt, Peter Bell, Andreas Maier, and Vincent Christlein. 2020. Enhancing Human Pose Estimation in Ancient Vase Paintings via Perceptually-grounded Style Transfer Learning. *arXiv preprint arXiv:2012.05616* (2020).
- [151] Naureen Mahmood, Nima Ghorbani, Nikolaus F. Troje, Gerard Pons-Moll, and Michael J. Black. 2019. AMASS: Archive of Motion Capture as Surface Shapes. In *ICCV*.
- [152] Weian Mao, Yongtao Ge, Chunhua Shen, Zhi Tian, Xinlong Wang, and Zhibin Wang. 2021. Tfpose: Direct human pose estimation with transformers. *arXiv preprint arXiv:2103.15320* (2021).
- [153] Weian Mao, Yongtao Ge, Chunhua Shen, Zhi Tian, Xinlong Wang, Zhibin Wang, and Anton van den Hengel. 2022. Poseur: Direct Human Pose Regression with Transformers. *arXiv preprint arXiv:2201.07412* (2022).
- [154] Amir Markovitz, Gilad Sharir, Itamar Friedman, Lih Zelnik-Manor, and Shai Avidan. 2020. Graph Embedded Pose Clustering for Anomaly Detection. In *CVPR*.
- [155] Julieta Martinez, Rayat Hossain, Javier Romero, and James J. Little. 2017. A simple yet effective baseline for 3d human pose estimation. In *ICCV*.
- [156] D. Mehta, H. Rhodin, D. Casas, P. Fua, O. Sotnychenko, W. Xu, and C. Theobalt. 2017. Monocular 3D Human Pose Estimation in the Wild Using Improved CNN Supervision. In *3DV*.
- [157] Dushyant Mehta, Oleksandr Sotnychenko, Franziska Mueller, Weipeng Xu, Mohamed Elgharib, Pascal Fua, Hans-Peter Seidel, Helge Rhodin, Gerard Pons-Moll, and Christian Theobalt. 2020. XNect: Real-time Multi-Person 3D Motion Capture with a Single RGB Camera. *ACM TOG* (2020).
- [158] Dushyant Mehta, Oleksandr Sotnychenko, Franziska Mueller, Weipeng Xu, Srinath Sridhar, Gerard Pons-Moll, and Christian Theobalt. 2018. Single-Shot Multi-Person 3D Pose Estimation From Monocular RGB. In *3DV*.
- [159] Dushyant Mehta, Srinath Sridhar, Oleksandr Sotnychenko, Helge Rhodin, Mohammad Shafiei, Hans-Peter Seidel, et al. 2017. Vnect: Real-time 3d human pose estimation with a single rgb camera. *ACM TOG* (2017).
- [160] Antonio S Micilotta, Eng-Jon Ong, and Richard Bowden. 2006. Real-time upper body detection and 3D pose estimation in monoscopic images. In *ECCV*.
- [161] Rahul Mitra, Nitesh B. Gundavarapu, Abhishek Sharma, and Arjun Jain. 2020. Multiview-Consistent Semi-Supervised Learning for 3D Human Pose Estimation. In *CVPR*.
- [162] Thomas B Moeslund and Erik Granum. 2001. A survey of computer vision-based human motion capture. *CVIU* (2001).
- [163] Thomas B Moeslund, Adrian Hilton, and Volker Krüger. 2006. A survey of advances in vision-based human motion capture and analysis. *CVIU* (2006).
- [164] Gyeongsik Moon, Juyong Chang, and Kyoung Mu Lee. 2019. Camera Distance-aware Top-down Approach for 3D Multi-person Pose Estimation from a Single RGB Image. In *ICCV*.
- [165] Gyeongsik Moon, Ju Yong Chang, and Kyoung Mu Lee. 2019. Posefix: Model-agnostic general human pose refinement network. In *CVPR*.
- [166] Gyeongsik Moon and Kyoung Mu Lee. 2020. I2L-MeshNet: Image-to-Lixel Prediction Network for Accurate 3D Human Pose and Mesh Estimation from a Single RGB Image. In *ECCV*.

- [167] Francesc Moreno-Noguer. 2017. 3d human pose estimation from a single image via distance matrix regression. In *CVPR*.
- [168] Tewodros Legesse Munea, Yalew Zelalem Jembre, Halefom Tekle Weldegebriel, Longbiao Chen, Chenxi Huang, and Chenhui Yang. 2020. The Progress of Human Pose Estimation: A Survey and Taxonomy of Models Applied in 2D Human Pose Estimation. *IEEE Access* (2020).
- [169] Alejandro Newell, Zhiao Huang, and Jia Deng. 2017. Associative embedding: End-to-end learning for joint detection and grouping. In *NeurIPS*.
- [170] Alejandro Newell, Kaiyu Yang, and Jia Deng. 2016. Stacked hourglass networks for human pose estimation. In *ECCV*.
- [171] Aiden Nibali, Zhen He, Stuart Morgan, and Luke Prendergast. 2018. Numerical coordinate regression with convolutional neural networks. *arXiv preprint arXiv:1801.07372* (2018).
- [172] B. X. Nie, P. Wei, and S. Zhu. 2017. Monocular 3D Human Pose Estimation by Predicting Depth on Joints. In *ICCV*.
- [173] Qiang Nie, Ziwei Liu, and Yunhui Liu. 2020. Unsupervised Human 3D Pose Representation with Viewpoint and Pose Disentanglement. In *ECCV*.
- [174] Xuecheng Nie, Jiashi Feng, Jianfeng Zhang, and Shuicheng Yan. 2019. Single-Stage Multi-Person Pose Machines. In *ICCV*.
- [175] Mohamed Omran, Christoph Lassner, Gerard Pons-Moll, Peter V. Gehler, and Bernt Schiele. 2018. Neural Body Fitting: Unifying Deep Learning and Model-Based Human Pose and Shape Estimation. In *3DV*.
- [176] Ahmed A A Osman, Timo Bolkart, and Michael J. Black. 2020. STAR: A Spare Trained Articulated Human Body Regressor. In *ECCV*.
- [177] Paschalis Panteleris and Antonis Argyros. 2021. PE-former: Pose Estimation Transformer. *arXiv preprint arXiv:2112.04981* (2021).
- [178] George Papandreou, Tyler Zhu, Liang-Chieh Chen, Spyros Gidaris, Jonathan Tompson, and Kevin Murphy. 2018. Personlab: Person pose estimation and instance segmentation with a bottom-up, part-based, geometric embedding model. In *ECCV*.
- [179] George Papandreou, Tyler Zhu, Nori Kanazawa, Alexander Toshev, Jonathan Tompson, Chris Bregler, and Kevin Murphy. 2017. Towards Accurate Multi-Person Pose Estimation in the Wild. In *CVPR*.
- [180] Chaitanya Patel, Zhouyingcheng Liao, and Gerard Pons-Moll. 2020. TailorNet: Predicting Clothing in 3D as a Function of Human Pose, Shape and Garment Style. In *CVPR*.
- [181] Georgios Pavlakos, Vasileios Choutas, Nima Ghorbani, Timo Bolkart, Ahmed A. A. Osman, Dimitrios Tzionas, and Michael J. Black. 2019. Expressive Body Capture: 3D Hands, Face, and Body from a Single Image. In *CVPR*.
- [182] Georgios Pavlakos, Xiaowei Zhou, and Kostas Daniilidis. 2018. Ordinal Depth Supervision for 3D Human Pose Estimation. In *CVPR*.
- [183] Georgios Pavlakos, Xiaowei Zhou, Konstantinos G Derpanis, and Kostas Daniilidis. 2017. Coarse-to-Fine Volumetric Prediction for Single-Image 3D Human Pose. In *CVPR*.
- [184] Georgios Pavlakos, Xiaowei Zhou, Konstantinos G. Derpanis, and Kostas Daniilidis. 2017. Harvesting Multiple Views for Marker-Less 3D Human Pose Annotations. In *CVPR*.
- [185] Georgios Pavlakos, Luyang Zhu, Xiaowei Zhou, and Kostas Daniilidis. 2018. Learning to Estimate 3D Human Pose and Shape from a Single Color Image. In *CVPR*.
- [186] Dario Pavlo, Christoph Feichtenhofer, David Grangier, and Michael Auli. 2019. 3D human pose estimation in video with temporal convolutions and semi-supervised training. In *CVPR*.
- [187] Xi Peng, Zhiqiang Tang, Fei Yang, Rogerio S Feris, and Dimitris Metaxas. 2018. Jointly optimize data augmentation and network training: Adversarial data augmentation in human pose estimation. In *CVPR*.
- [188] Tomas Pfister, James Charles, and Andrew Zisserman. 2015. Flowing convnets for human pose estimation in videos. In *ICCV*.
- [189] Tomas Pfister, Karen Simonyan, James Charles, and Andrew Zisserman. 2014. Deep convolutional neural networks for efficient pose estimation in gesture videos. In *ACCV*.
- [190] Aleksis Pirinen, Erik Gärtner, and Cristian Sminchisescu. 2019. Domes to Drones: Self-Supervised Active Triangulation for 3D Human Pose Reconstruction. In *NeurIPS*.
- [191] Leonid Pishchulin, Eldar Insafutdinov, Siyu Tang, Bjoern Andres, Mykhaylo Andriluka, Peter V Gehler, and Bernt Schiele. 2016. Deepcut: Joint subset partition and labeling for multi person pose estimation. In *CVPR*.
- [192] Gerard Pons-Moll, Javier Romero, Naureen Mahmood, and Michael J. Black. 2015. Dyna: A Model of Dynamic Human Shape in Motion. *ACM TOG* (2015).
- [193] Ronald Poppe. 2007. Vision-based human motion analysis: An overview. *CVIU* (2007).
- [194] Ammar Qammar and Antonis A Argyros. 2019. MocapNET: Ensemble of SNN Encoders for 3D Human Pose Estimation in RGB Images.. In *BMVC*.
- [195] Charles R Qi, Hao Su, Kaichun Mo, and Leonidas J Guibas. 2017. Pointnet: Deep learning on point sets for 3d classification and segmentation. In *CVPR*.

- [196] Charles Ruizhongtai Qi, Li Yi, Hao Su, and Leonidas J Guibas. 2017. Pointnet++: Deep hierarchical feature learning on point sets in a metric space. In *NeurIPS*.
- [197] Haibo Qiu, Chunyu Wang, Jingdong Wang, Naiyan Wang, and Wenjun Zeng. 2019. Cross View Fusion for 3D Human Pose Estimation. In *ICCV*.
- [198] Lingteng Qiu, Xuanye Zhang, Yanran Li, Guanbin Li, Xiaojun Wu, Zixiang Xiong, Xiaoguang Han, and Shuguang Cui. 2020. Peeking into occluded joints: A novel framework for crowd pose estimation. *arXiv preprint arXiv:2003.10506* (2020).
- [199] Varun Ramakrishna, Daniel Munoz, Martial Hebert, James Andrew Bagnell, and Yaser Sheikh. 2014. Pose machines: Articulated pose estimation via inference machines. In *ECCV*.
- [200] Mir Rayat Imtiaz Hossain and James J. Little. 2018. Exploiting temporal information for 3D human pose estimation. In *ECCV*.
- [201] N Dinesh Reddy, Laurent Guigues, Leonid Pishchulin, Jayan Eledath, and Srinivasa G Narasimhan. 2021. TesseTrack: End-to-End Learnable Multi-Person Articulated 3D Pose Tracking. In *CVPR*. 15190–15200.
- [202] Edoardo Remelli, Shangchen Han, Sina Honari, Pascal Fua, and Robert Wang. 2020. Lightweight Multi-View 3D Pose Estimation Through Camera-Disentangled Representation. In *CVPR*.
- [203] Shaoqing Ren, Kaiming He, Ross Girshick, and Jian Sun. 2016. Faster r-cnn: Towards real-time object detection with region proposal networks. *IEEE TPAMI* (2016).
- [204] Helge Rhodin, Mathieu Salzmann, and Pascal Fua. 2018. Unsupervised Geometry-Aware Representation for 3D Human Pose Estimation. In *ECCV*.
- [205] Helge Rhodin, Jörg Spörri, Isinsu Katircioglu, Victor Constantin, Frédéric Meyer, Erich Müller, Mathieu Salzmann, and Pascal Fua. 2018. Learning Monocular 3D Human Pose Estimation From Multi-View Images. In *CVPR*.
- [206] G. Rogez, P. Weinzaepfel, and C. Schmid. 2017. LCR-Net: Localization-Classification-Regression for Human Pose. In *CVPR*.
- [207] Grégory Rogez, Philippe Weinzaepfel, and Cordelia Schmid. 2019. LCR-Net++: Multi-person 2D and 3D Pose Detection in Natural Images. *IEEE TPAMI* (2019).
- [208] Sebastian Ruder. 2017. An overview of multi-task learning in deep neural networks. *arXiv preprint arXiv:1706.05098* (2017).
- [209] Nitin Saini, Eric Price, Rahul Tallamraju, Raffi Enfiaciaud, Roman Ludwig, Igor Martinović, Aamir Ahmad, and Michael Black. 2019. Markerless Outdoor Human Motion Capture Using Multiple Autonomous Micro Aerial Vehicles. In *ICCV*.
- [210] Shunsuke Saito, Zeng Huang, Ryota Natsume, Shigeo Morishima, Angjoo Kanazawa, and Hao Li. 2019. PIFu: Pixel-Aligned Implicit Function for High-Resolution Clothed Human Digitization. In *ICCV*.
- [211] Shunsuke Saito, Tomas Simon, Jason Saragih, and Hanbyul Joo. 2020. PIFuHD: Multi-Level Pixel-Aligned Implicit Function for High-Resolution 3D Human Digitization. In *CVPR*.
- [212] Ben Sapp and Ben Taskar. 2013. Modc: Multimodal decomposable models for human pose estimation. In *CVPR*.
- [213] Nikolaos Sarafianos, Bogdan Boteanu, Bogdan Ionescu, and Ioannis A Kakadiaris. 2016. 3d human pose estimation: A review of the literature and analysis of covariates. *CVIU* (2016).
- [214] Saurabh Sharma, Pavan Teja Varigonda, Prashast Bindal, Abhishek Sharma, and Arjun Jain. 2019. Monocular 3D Human Pose Estimation by Generation and Ordinal Ranking. In *ICCV*.
- [215] L. Sigal, A. Balan, and M. J. Black. 2010. HumanEva: Synchronized video and motion capture dataset and baseline algorithm for evaluation of articulated human motion. *IJCV* (2010).
- [216] Kai Su, Dongdong Yu, Zhenqi Xu, Xin Geng, and Changhu Wang. 2019. Multi-person pose estimation with enhanced channel-wise and spatial information. In *CVPR*.
- [217] Jennifer J. Sun, Jiaping Zhao, Liang-Chieh Chen, Florian Schroff, Hartwig Adam, and Ting Liu. 2020. View-Invariant Probabilistic Embedding for Human Pose. In *ECCV*.
- [218] Ke Sun, Bin Xiao, Dong Liu, and Jingdong Wang. 2019. Deep high-resolution representation learning for human pose estimation. In *CVPR*.
- [219] Xiao Sun, Jiaxiang Shang, Shuang Liang, and Yichen Wei. 2017. Compositional human pose regression. In *ICCV*.
- [220] Christian Szegedy, Wei Liu, Yangqing Jia, Pierre Sermanet, Scott Reed, Dragomir Anguelov, Dumitru Erhan, Vincent Vanhoucke, and Andrew Rabinovich. 2015. Going deeper with convolutions. In *CVPR*.
- [221] Wei Tang and Ying Wu. 2019. Does Learning Specific Features for Related Parts Help Human Pose Estimation?. In *CVPR*.
- [222] Wei Tang, Pei Yu, and Ying Wu. 2018. Deeply learned compositional models for human pose estimation. In *ECCV*.
- [223] Bugra Tekin, Isinsu Katircioglu, Mathieu Salzmann, Vincent Lepetit, and Pascal Fua. 2016. Structured Prediction of 3D Human Pose with Deep Neural Networks. In *BMVC*.
- [224] Bugra Tekin, Pablo Márquez-Neila, Mathieu Salzmann, and Pascal Fua. 2017. Learning to fuse 2d and 3d image cues for monocular body pose estimation. In *ICCV*.

- [225] Bugra Tekin, Artem Rozantsev, Vincent Lepetit, and Pascal Fua. 2016. Direct Prediction of 3D Body Poses From Motion Compensated Sequences. In *CVPR*.
- [226] Zhi Tian, Hao Chen, and Chunhua Shen. 2019. DirectPose: Direct End-to-End Multi-Person Pose Estimation. *arXiv preprint arXiv:1911.07451* (2019).
- [227] Denis Tome, Thiemo Alldieck, Patrick Peluse, Gerard Pons-Moll, Lourdes Agapito, Hernan Badino, and Fernando De la Torre. 2020. SelfPose: 3D Egocentric Pose Estimation from a Headset Mounted Camera. *arXiv preprint arXiv:2011.01519*.
- [228] Denis Tome, Patrick Peluse, Lourdes Agapito, and Hernan Badino. 2019. xR-EgoPose: Egocentric 3D Human Pose from an HMD Camera. In *ICCV*.
- [229] Jonathan Tompson, Ross Goroshin, Arjun Jain, Yann LeCun, and Christoph Bregler. 2015. Efficient object localization using convolutional networks. In *CVPR*.
- [230] Jonathan J Tompson, Arjun Jain, Yann LeCun, and Christoph Bregler. 2014. Joint training of a convolutional network and a graphical model for human pose estimation. In *NeurIPS*.
- [231] Alexander Toshev and Christian Szegedy. 2014. Deeppose: Human pose estimation via deep neural networks. In *CVPR*.
- [232] Matt Trumble, Andrew Gilbert, Charles Malleson, Adrian Hilton, and John Collomosse. 2017. Total Capture: 3D Human Pose Estimation Fusing Video and Inertial Sensors. In *BMVC*.
- [233] Hanyue Tu, Chunyu Wang, and Wenjun Zeng. 2020. VoxelPose: Towards Multi-Camera 3D Human Pose Estimation in Wild Environment. In *ECCV*.
- [234] Hsiao-Yu Fish Tung, Hsiao-Wei Tung, Ersin Yumer, and Katerina Fragkiadaki. 2017. Self-Supervised Learning of Motion Capture. In *NeurIPS*.
- [235] Rafi Umer, Andreas Doering, Bastian Leibe, and Juergen Gall. 2020. Self-supervised Keypoint Correspondences for Multi-Person Pose Estimation and Tracking in Videos. *arXiv preprint arXiv:2004.12652* (2020).
- [236] Raquel Urtasun and Pascal Fua. 2004. 3D human body tracking using deterministic temporal motion models. In *ECCV*.
- [237] Gul Varol, Javier Romero, Xavier Martin, Naureen Mahmood, Michael J Black, Ivan Laptev, and Cordelia Schmid. 2017. Learning from synthetic humans. In *CVPR*.
- [238] Ashish Vaswani, Noam Shazeer, Niki Parmar, Jakob Uszkoreit, Llion Jones, Aidan N Gomez, Łukasz Kaiser, and Illia Polosukhin. 2017. Attention is all you need. In *Advances in neural information processing systems*. 5998–6008.
- [239] Ignas Budvytis Vince Tan and Roberto Cipolla. 2017. Indirect deep structured learning for 3D human body shape and pose prediction. In *BMVC*.
- [240] Timo von Marcard, Roberto Henschel, Michael J. Black, Bodo Rosenhahn, and Gerard Pons-Moll. 2018. Recovering Accurate 3D Human Pose in The Wild Using IMUs and a Moving Camera. In *ECCV*.
- [241] Timo Von Marcard, Bodo Rosenhahn, Michael J Black, and Gerard Pons-Moll. 2017. Sparse inertial poser: Automatic 3d human pose estimation from sparse imus. In *Computer Graphics Forum*.
- [242] Bastian Wandt and Bodo Rosenhahn. 2019. RepNet: Weakly Supervised Training of an Adversarial Reprojection Network for 3D Human Pose Estimation. In *CVPR*.
- [243] Haoyang Wang, Riza Alp Guler, Iasonas Kokkinos, George Papandreou, and Stefanos Zafeiriou. 2020. BLSM: A Bone-Level Skinned Model of the Human Mesh. In *ECCV*.
- [244] Jue Wang, Shaoli Huang, Xinchao Wang, and Dacheng Tao. 2019. Not All Parts Are Created Equal: 3D Pose Estimation by Modeling Bi-Directional Dependencies of Body Parts. In *ICCV*.
- [245] Jian Wang, Xiang Long, Yuan Gao, Errui Ding, and Shilei Wen. 2020. Graph-PCNN: Two Stage Human Pose Estimation with Graph Pose Refinement. *arXiv preprint arXiv:2007.10599* (2020).
- [246] Jianbo Wang, Kai Qiu, Houwen Peng, Jianlong Fu, and Jianke Zhu. 2019. AI Coach: Deep Human Pose Estimation and Analysis for Personalized Athletic Training Assistance. In *ACM MM*.
- [247] Jingbo Wang, Sijie Yan, Yuanjun Xiong, and Dahua Lin. 2020. Motion Guided 3D Pose Estimation from Videos. In *ECCV*.
- [248] Kangkan Wang, Jin Xie, Guofeng Zhang, Lei Liu, and Jian Yang. 2020. Sequential 3D Human Pose and Shape Estimation From Point Clouds. In *CVPR*.
- [249] Min Wang, Xipeng Chen, Wentao Liu, Chen Qian, Liang Lin, and Lizhuang Ma. 2018. DRPose3D: Depth Ranking in 3D Human Pose Estimation. In *IJCAI*.
- [250] Tao Wang, Jianfeng Zhang, Yujun Cai, Shuicheng Yan, and Jiashi Feng. 2021. Direct Multi-view Multi-person 3D Human Pose Estimation. *Advances in Neural Information Processing Systems* (2021).
- [251] Shih-En Wei, Varun Ramakrishna, Takeo Kanade, and Yaser Sheikh. 2016. Convolutional pose machines. In *CVPR*.
- [252] C. Weng, B. Curless, and I. Kemelmacher-Shlizerman. 2019. Photo Wake-Up: 3D Character Animation From a Single Photo. In *CVPR*.

- [253] Nora S Willett, Hijung Valentina Shin, Zeyu Jin, Wilmot Li, and Adam Finkelstein. 2020. Pose2Pose: pose selection and transfer for 2D character animation. In *IUI*.
- [254] Jiahong Wu, He Zheng, Bo Zhao, Yixin Li, Baoming Yan, Rui Liang, Wenjia Wang, Shipai Zhou, et al. 2017. Ai challenger: A large-scale dataset for going deeper in image understanding. *arXiv preprint arXiv:1711.06475* (2017).
- [255] Donglai Xiang, Hanbyul Joo, and Yaser Sheikh. 2019. Monocular total capture: Posing face, body, and hands in the wild. In *CVPR*.
- [256] Bin Xiao, Haiping Wu, and Yichen Wei. 2018. Simple Baselines for Human Pose Estimation and Tracking. In *ECCV*.
- [257] Rongchang Xie, Chunyu Wang, and Yizhou Wang. 2020. MetaFuse: A Pre-trained Fusion Model for Human Pose Estimation. In *CVPR*.
- [258] Fu Xiong, Boshen Zhang, Yang Xiao, Zhiguo Cao, Taidong Yu, Joey Zhou Tianyi, and Junsong Yuan. 2019. A2J: Anchor-to-Joint Regression Network for 3D Articulated Pose Estimation from a Single Depth Image. In *ICCV*.
- [259] Hongyi Xu, Eduard Gabriel Bazavan, Andrei Zanfir, William T. Freeman, Rahul Sukthankar, and Cristian Sminchisescu. 2020. GHUM & GHUML: Generative 3D Human Shape and Articulated Pose Models. In *CVPR*.
- [260] Jingwei Xu, Zhenbo Yu, Bingbing Ni, Jiancheng Yang, Xiaokang Yang, and Wenjun Zhang. 2020. Deep Kinematics Analysis for Monocular 3D Human Pose Estimation. In *CVPR*.
- [261] Weipeng Xu, Avishek Chatterjee, Michael Zollhoefer, Helge Rhodin, Pascal Fua, Hans-Peter Seidel, and Christian Theobalt. 2019. Mo 2 cap 2: Real-time mobile 3d motion capture with a cap-mounted fisheye camera. *IEEE T VIS COMPUT GR* (2019).
- [262] Xiangyu Xu, Hao Chen, Francesc Moreno-Noguer, Laszlo A. Jeni, and Fernando De la Torre. 2020. 3D Human Shape and Pose from a Single Low-Resolution Image with Self-Supervised Learning. In *ECCV*.
- [263] Sijie Yan, Yuanjun Xiong, and Dahua Lin. 2018. Spatial temporal graph convolutional networks for skeleton-based action recognition. In *AAAI*.
- [264] Sen Yang, Zhibin Quan, Mu Nie, and Wankou Yang. 2021. Transpose: Keypoint localization via transformer. In *ICCV*.
- [265] Wei Yang, Shuang Li, Wanli Ouyang, Hongsheng Li, and Xiaogang Wang. 2017. Learning feature pyramids for human pose estimation. In *ICCV*.
- [266] Wei Yang, Wanli Ouyang, Hongsheng Li, and Xiaogang Wang. 2016. End-to-end learning of deformable mixture of parts and deep convolutional neural networks for human pose estimation. In *CVPR*.
- [267] Wei Yang, Wanli Ouyang, Xiaolong Wang, Jimmy Ren, Hongsheng Li, and Xiaogang Wang. 2018. 3D Human Pose Estimation in the Wild by Adversarial Learning. In *CVPR*.
- [268] Yi Yang and Deva Ramanan. 2012. Articulated human detection with flexible mixtures of parts. *IEEE TPAMI* (2012).
- [269] T. Yu, J. Zhao, Z. Zheng, K. Guo, Q. Dai, H. Li, G. Pons-Moll, and Y. Liu. 2019. DoubleFusion: Real-time Capture of Human Performances with Inner Body Shapes from a Single Depth Sensor. *IEEE TPAMI* (2019).
- [270] Tao Yu, Zerong Zheng, Yuan Zhong, Jianhui Zhao, Qionghai Dai, Gerard Pons-Moll, and Yebin Liu. 2019. Simulcap: Single-view human performance capture with cloth simulation. In *CVPR*.
- [271] Andrei Zanfir, Eduard Gabriel Bazavan, Hongyi Xu, Bill Freeman, Rahul Sukthankar, and Cristian Sminchisescu. 2020. Weakly Supervised 3D Human Pose and Shape Reconstruction with Normalizing Flows. In *ECCV*.
- [272] A. Zanfir, E. Marinou, and C. Sminchisescu. 2018. Monocular 3D Pose and Shape Estimation of Multiple People in Natural Scenes: The Importance of Multiple Scene Constraints. In *CVPR*.
- [273] Andrei Zanfir, Elisabeta Marinou, Mihai Zanfir, Alin-Ionut Popa, and Cristian Sminchisescu. 2018. Deep Network for the Integrated 3D Sensing of Multiple People in Natural Images. In *NeurIPS*.
- [274] Ailing Zeng, Xiao Sun, Fuyang Huang, Minhao Liu, Qiang Xu, and Stephen Lin. 2020. SRNet: Improving Generalization in 3D Human Pose Estimation with a Split-and-Recombine Approach. In *ECCV*.
- [275] W. Zeng, W. Ouyang, P. Luo, W. Liu, and X. Wang. 2020. 3D Human Mesh Regression With Dense Correspondence. In *CVPR*.
- [276] Feng Zhang, Xiatian Zhu, Hanbin Dai, Mao Ye, and Ce Zhu. 2020. Distribution-aware coordinate representation for human pose estimation. In *CVPR*.
- [277] Feng Zhang, Xiatian Zhu, and Mao Ye. 2019. Fast human pose estimation. In *CVPR*.
- [278] Hong Zhang, Hao Ouyang, Shu Liu, Xiaojuan Qi, Xiaoyong Shen, Ruigang Yang, and Jiaya Jia. 2019. Human pose estimation with spatial contextual information. *arXiv preprint arXiv:1901.01760* (2019).
- [279] Haotian Zhang, Cristobal Scutto, Maneesh Agrawala, and Kayvon Fatahalian. 2020. Vid2Player: Controllable Video Sprites that Behave and Appear like Professional Tennis Players. *arXiv preprint arXiv:2008.04524* (2020).
- [280] Hongwen Zhang, Yating Tian, Xinchu Zhou, Wanli Ouyang, Yebin Liu, Limin Wang, and Zhenan Sun. 2021. PyMAF: 3D Human Pose and Shape Regression with Pyramidal Mesh Alignment Feedback Loop. In *ICCV*.
- [281] Tianshu Zhang, Buzhen Huang, and Yangang Wang. 2020. Object-Occluded Human Shape and Pose Estimation From a Single Color Image. In *CVPR*.
- [282] Wenqiang Zhang, Jiemin Fang, Xinggang Wang, and Wenyu Liu. 2020. EfficientPose: Efficient Human Pose Estimation with Neural Architecture Search. *arXiv preprint arXiv:2012.07086* (2020).

- [283] Weiyu Zhang, Menglong Zhu, and Konstantinos G Derpanis. 2013. From actemes to action: A strongly-supervised representation for detailed action understanding. In *ICCV*.
- [284] Yuxiang Zhang, Liang An, Tao Yu, Xiu Li, Kun Li, and Yebin Liu. 2020. 4D Association Graph for Realtime Multi-person Motion Capture Using Multiple Video Cameras. In *CVPR*.
- [285] Yuexi Zhang, Yin Wang, Octavia Camps, and Mario Sznaier. 2020. Key Frame Proposal Network for Efficient Pose Estimation in Videos. *arXiv preprint arXiv:2007.15217* (2020).
- [286] Zhe Zhang, Chunyu Wang, Wenhui Qin, and Wenjun Zeng. 2020. Fusing Wearable IMUs With Multi-View Images for Human Pose Estimation: A Geometric Approach. In *CVPR*.
- [287] Zhe Zhang, Chunyu Wang, Weichao Qiu, Wenhui Qin, and Wenjun Zeng. 2020. AdaFuse: Adaptive Multiview Fusion for Accurate Human Pose Estimation in the Wild. *IJCV* (2020).
- [288] Long Zhao, Xi Peng, Yu Tian, Mubbasir Kapadia, and Dimitris N. Metaxas. 2019. Semantic Graph Convolutional Networks for 3D Human Pose Regression. In *CVPR*.
- [289] Mingmin Zhao, Yingcheng Liu, Aniruddh Raghu, Tianhong Li, Hang Zhao, Antonio Torralba, and Dina Katabi. 2019. Through-Wall Human Mesh Recovery Using Radio Signals. In *ICCV*.
- [290] Mingmin Zhao, Yonglong Tian, Hang Zhao, Mohammad Abu Alsheikh, Tianhong Li, Rumen Hristov, Zachary Kabelac, Dina Katabi, and Antonio Torralba. 2018. RF-based 3D skeletons. In *SIGCOMM 2018*.
- [291] Weixi Zhao, Yunjie Tian, Qixiang Ye, Jianbin Jiao, and Weiqiang Wang. 2021. GraFormer: Graph Convolution Transformer for 3D Pose Estimation. *arXiv preprint arXiv:2109.08364* (2021).
- [292] Jianan Zhen, Qi Fang, Jiaming Sun, Wentao Liu, Wei Jiang, Hujun Bao, and Xiaowei Zhou. 2020. SMAP: Single-Shot Multi-Person Absolute 3D Pose Estimation. In *ECCV*.
- [293] Ce Zheng, Matias Mendieta, Pu Wang, Aidong Lu, and Chen Chen. 2021. A Lightweight Graph Transformer Network for Human Mesh Reconstruction from 2D Human Pose. *arXiv preprint arXiv:2111.12696* (2021).
- [294] Ce Zheng, Sijie Zhu, Matias Mendieta, Taojiannan Yang, Chen Chen, and Zhengming Ding. 2021. 3D Human Pose Estimation with Spatial and Temporal Transformers. *ICCV* (2021).
- [295] Tiancheng Zhi, Christoph Lassner, Tony Tung, Carsten Stoll, Srinivasa G. Narasimhan, and Minh Vo. 2020. TexMesh: Reconstructing Detailed Human Texture and Geometry from RGB-D Video. In *ECCV*.
- [296] Keyang Zhou, Bharat Lal Bhatnagar, and Gerard Pons-Moll. 2020. Unsupervised Shape and Pose Disentanglement for 3D Meshes. *arXiv preprint arXiv:2007.11341* (2020).
- [297] K. Zhou, X. Han, N. Jiang, K. Jia, and J. Lu. 2019. HEMlets Pose: Learning Part-Centric Heatmap Triplets for Accurate 3D Human Pose Estimation. In *ICCV*.
- [298] Xingyi Zhou, Qixing Huang, Xiao Sun, Xiangyang Xue, and Yichen Wei. 2017. Towards 3D Human Pose Estimation in the Wild: A Weakly-Supervised Approach. In *ICCV*.
- [299] Xingyi Zhou, Xiao Sun, Wei Zhang, Shuang Liang, and Yichen Wei. 2016. Deep kinematic pose regression. In *ECCV*.
- [300] Xingyi Zhou, Dequan Wang, and Philipp Krähenbühl. 2019. Objects as points. *arXiv preprint arXiv:1904.07850* (2019).
- [301] Xiaowei Zhou, Menglong Zhu, Kosta Derpanis, and Kostas Daniilidis. 2016. Sparseness Meets Deepness: 3D Human Pose Estimation from Monocular Video. In *CVPR*.
- [302] Xiaowei Zhou, Menglong Zhu, Georgios Pavlakos, Spyridon Leonardos, Konstantinos G Derpanis, and Kostas Daniilidis. 2018. Monocap: Monocular human motion capture using a cnn coupled with a geometric prior. *IEEE TPAMI*.
- [303] Hao Zhu, Xinxin Zuo, Sen Wang, Xun Cao, and Ruigang Yang. 2019. Detailed human shape estimation from a single image by hierarchical mesh deformation. In *CVPR*.
- [304] Luyang Zhu, Konstantinos Rematas, Brian Curless, Steve Seitz, and Ira Kemelmacher-Shlizerman. 2020. Reconstructing NBA players. In *ECCV*.
- [305] Xiangyu Zhu, Yingying Jiang, and Zhenbo Luo. 2017. Multi-person pose estimation for posetrack with enhanced part affinity fields. In *ICCV PoseTrack Workshop*.
- [306] Zhiming Zou and Wei Tang. 2021. Modulated Graph Convolutional Network for 3D Human Pose Estimation. In *ICCV*. 11477–11487.
- [307] Silvia Zuffi and Michael J. Black. 2015. The Stitched Puppet: A Graphical Model of 3D Human Shape and Pose. In *CVPR*.
- [308] Silvia Zuffi, Oren Freifeld, and Michael J Black. 2012. From pictorial structures to deformable structures. In *CVPR*.